Adaptive Federated Optimization

Sashank J. Reddi[*]
Google Research
sashank@google.com

Zachary Charles[*]
Google Research
zachcharles@google.com

Manzil Zaheer
Google Research
manzilzaheer@google.com

Zachary Garrett
Google Research
zachgarrett@google.com

Keith Rush
Google Research
krush@google.com

Jakub Konečný
Google Research
konkey@google.com

Sanjiv Kumar
Google Research
sanjivk@google.com

H. Brendan McMahan
Google Research
mcmahan@google.com

Abstract

Federated learning is a distributed machine learning paradigm in which a large number of clients coordinate with a central server to learn a model without sharing their own training data. Due to the heterogeneity of the client datasets, standard federated optimization methods such as Federated Averaging (FEDAVG) are often difficult to tune and exhibit unfavorable convergence behavior. In non-federated settings, adaptive optimization methods have had notable success in combating such issues. In this work, we propose federated versions of adaptive optimizers, including ADAGRAD, ADAM, and YOGI, and analyze their convergence in the presence of heterogeneous data for general nonconvex settings. Our results highlight the interplay between client heterogeneity and communication efficiency. We also perform extensive experiments on these methods and show that the use of adaptive optimizers can significantly improve the performance of federated learning.

1 Introduction

Federated learning (FL) is a machine learning paradigm in which multiple clients (such as edge devices, or separate organizations) cooperate to learn a model under the orchestration of a central server (McMahan et al., 2017). The core tenet of FL is that raw client data is never shared with the server or among distinct clients. This distinguishes FL from traditional distributed optimization, as these restrictions require FL to contend with *heterogeneous data*. For a more in-depth discussion of the challenges involved, we defer to Kairouz et al. (2019) and Li et al. (2019a).

Standard optimization methods, such as mini-batch SGD, are often unsuitable in FL and can incur high communication costs. To this end, many federated optimization methods utilize *local client updates*, in which clients update their models multiple times before communicating to synchronize models. This can greatly reduce the amount of communication required to train a model. One popular such method is FEDAVG (McMahan et al., 2017). In each round of FEDAVG, a small subset of the clients locally perform some number of epochs of SGD. The clients then communicate their model updates to the server, which averages them to compute a new global model.

While FEDAVG has seen remarkable success, recent works have highlighted drawbacks of the method (Karimireddy et al., 2019; Hsu et al., 2019). In this paper, we focus on two issues: (a) *client drift* and (b) lack of *adaptive learning rates* during optimization. In heterogeneous settings, multiple local SGD epochs can cause clients to drift away from a globally optimal model. For instance, the extreme case where each client *exactly* minimizes the loss over its local data using SGD and the server averages the models is equivalent to *one-shot averaging*, which is known to fail in heterogeneous settings. Moreover, FEDAVG, which is similar in spirit to SGD, is typically unsuitable for settings which exhibit heavy-tail stochastic gradient noise distributions during training (Zhang et al., 2019). Such settings necessitate the use of adaptive learning rates, which incorporate knowledge of past iterations to perform more informed optimization. Due to the decentralized nature of FL, incorporating adaptive learning rates into FEDAVG is challenging.

In this paper, we use a simple approach to incorporate adaptivity into FL. We view FEDAVG under a general optimization framework in which (1) clients perform multiple epochs of model updates using some *client optimizer* to minimize the

---

[*]Authors contributed equally to this work.

loss on their local data, (2) the server updates the global model by applying a gradient-based *server optimizer* to the average of the clients' *model updates* in order to minimize the loss across clients. As we show later, FEDAVG is the special case where SGD is used as both client and server optimizer and the server learning rate is 1. This provides a natural way to decouple client and server learning rates in FEDAVG and allows the use of adaptive learning rates on both client and server, thereby providing a means to control client drift.

This generalization of FEDAVG is appealing due to its simplicity and its ability to seamlessly incorporate adaptivity in the optimization process by using adaptive optimizers as client or server optimizers. Building upon this framework, we develop novel adaptive optimization techniques for FL by using per-coordinate adaptive methods as server optimizers, with an aim towards reducing the number of communication rounds required to reach a desired performance level.

Main contributions In light of the above, we highlight the main contributions of the paper.

- We study a general framework for optimization in FL using server and client optimizers. This framework generalizes many prior optimization methods for FL, including FEDAVG.

- Based on this framework, we propose adaptive optimization techniques for FL and provide convergence analysis in general nonconvex settings. To the best of our knowledge, these are the first methods for FL that use adaptive server optimization. We show an important interplay between the number of local steps and the amount of heterogeneity in the clients and quantify their effect on the convergence rates.

- We introduce comprehensive and reproducible empirical benchmarks for comparing FL optimization methods across a diverse and representative set of six FL tasks involving both image and text data. We use them to demonstrate the strong empirical performance of our adaptive optimizers and highlight the importance of coordinate-wise adaptivity. We see improved performance over FEDAVG on all six tasks, with dramatic improvements on four of them. We provide an open-source implementation of our adaptive optimizers, as well as code to reproduce our empirical results.[1]

Related work FEDAVG was first introduced by McMahan et al. (2017), which showed significant performance in federated learning. Many variants have since been proposed to tackle issues such as stability and client drift. Examples include methods that add a regularization term in the client objectives towards the broadcast model (Li et al., 2018), and methods that use momentum on the server (Hsu et al., 2019). Karimireddy et al. (2019) use control variates to reduce the client drift. While effective in some cases, the method requires clients to have state that persists throughout the training process, which is applicable only in some FL scenarios (Kairouz et al., 2019, Table 1). Xie et al. (2019) propose the use of adaptive client optimization for federated learning. While they show that it improves upon distributed versions of ADAGRAD, they generally do not compare it to FEDAVG.

When the clients are homogeneous, FEDAVG reduces to local SGD (Zinkevich et al., 2010), which has been analyzed theoretically by many works (Stich, 2019; Yu et al., 2019; Wang and Joshi, 2018; Stich and Karimireddy, 2019; Basu et al., 2019). In order to analyze FEDAVG in heterogeneous settings, many works derive convergence rates that depend on the amount of heterogeneity (Li et al., 2018; Wang et al., 2019; Khaled et al., 2019; Li et al., 2019b). The control variates used by Karimireddy et al. (2019) allow them to derive convergence rates independent of the amount of heterogeneity. For a more in-depth comparison, we defer to Kairouz et al. (2019).

There is a wide array of literature on the theoretical and empirical benefits of adaptive optimizers in non-federated settings, both in convex (McMahan and Streeter, 2010; Duchi et al., 2011; Kingma and Ba, 2015) and non-convex settings (Li and Orabona, 2018; Ward et al., 2018; Wu et al., 2019). Zaheer et al. (2018) study convergence failures of adaptive algorithms in non-convex settings, and develop an adaptive optimizer, YOGI, designed to improve convergence over methods such as ADAM. The aforementioned work focuses exclusively on non-federated optimization. Xie et al. (2019) give an analysis of an FL method that uses adaptive client optimization. However, this method requires twice as much communication as our methods, which use adaptive server optimization.

Notation For vectors $a, b \in \mathbb{R}^d$, we use $\sqrt{a}$ for element-wise square root, a^2 for element-wise square, a/b to denote element-wise division. For any vector $\theta_i \in \mathbb{R}^d$, either $\theta_{i,j}$ or $[\theta_i]_j$ are used to denote its jth coordinate.

---

[1]

2   Federated Learning and FEDAVG

In federated learning, we solve an optimization problem of the form:

$$\min_{x \in \mathbb{R}^d} f(x) = \frac{1}{m} \sum_{i=1}^m F_i(x), \tag{1}$$

where $F_i(x) = \mathbb{E}_{z \sim \mathcal{D}_i}[f_i(x, z)]$, is the loss function of the ith client, $z \in \mathcal{Z}$, and $\mathcal{D}_i$ is the data distribution for the ith client. For $i \neq j$, $\mathcal{D}_i$ and $\mathcal{D}_j$ may be very different. The functions F_i (and therefore f) may be nonconvex. For each i and x, we assume access to an *unbiased* stochastic gradient $g_i(x)$ of the client's true gradient $\nabla F_i(x)$. In addition, we make the following assumptions.

Assumption 1 (Lipschitz Gradient). *The function F_i is L-smooth for all $i \in [m]$ i.e., $\|\nabla F_i(x) - \nabla F_i(y)\| \leq L\|x-y\|$, for all $x, y \in \mathbb{R}^d$.*

Assumption 2 (Bounded Variance). *The function F_i have σ_l-bounded (local) variance i.e., $\mathbb{E}[\|\nabla[f_i(x,z)]_j - [\nabla F_i(x)]_j\|^2] = \sigma_{l,j}^2$ for all $x \in \mathbb{R}^d$, $j \in [d]$ and $i \in [m]$. Furthermore, we assume that the (global) variance is bounded, $(1/m) \sum_{i=1}^m \|\nabla[F_i(x)]_j - [\nabla f(x)]_j\|^2 \leq \sigma_{g,j}^2$ for all $x \in \mathbb{R}^d$ and $j \in [d]$.*

Assumption 3 (Bounded Gradients). *The function $f_i(x, z)$ have G-bounded gradients i.e., for any $i \in [m]$, $x \in \mathbb{R}^d$ and $z \in \mathcal{Z}$ we have $|[\nabla f_i(x,z)]_j| \leq G$ for all $j \in [d]$.*

With a slight abuse of notation, we use σ_l^2 and σ_g^2 to denote $\sum_{j=1}^d \sigma_{l,j}^2$ and $\sum_{j=1}^d \sigma_{g,j}^2$ respectively. Assumptions 1 and 3 are fairly standard in nonconvex optimization literature (Reddi et al., 2016; Ward et al., 2018; Zaheer et al., 2018). In this paper, we make no further assumptions regarding the similarity of different clients datasets. Assumption 2 assumes a form of bounded variance, but between the client objective functions and the overall objective function. This assumption has been used throughout various works on federated optimization (Li et al., 2018; Wang et al., 2019). Intuitively, the parameter σ_g signifies the similarity of the functions of different clients. In particular, the case of $\sigma_g = 0$ corresponds to the $i.i.d$ setting.

One of the most common approaches to solving (1) in federated settings is FEDAVG (McMahan et al., 2017) (see Algorithm 3 in the appendix). At each round of FEDAVG, a subset of clients are selected (typically randomly) and the server broadcasts its global model to each client. In parallel, the clients run SGD on their own loss function, and send the resulting model to the server. The server then updates its global model as the average of these local models.

Suppose that at round t, the server has model x_t and samples a set $\mathcal{S}$ of clients. Let x_i^t denote the model of each client $i \in \mathcal{S}$ after local training. We rewrite FEDAVG's update as

$$x_{t+1} = \frac{1}{|\mathcal{S}|} \sum_{i \in \mathcal{S}} x_i^t = x_t - \frac{1}{|\mathcal{S}|} \sum_{i \in \mathcal{S}} \left(x_t - x_i^t \right).$$

Let $\Delta_i^t := x_i^t - x_t$ and $\Delta_t = (1/|S|) \sum_{i \in \mathcal{S}} \Delta_i^t$. Then the server update in FEDAVG is equivalent to applying SGD to the "pseudo-gradient" $-\Delta_t$ with learning rate $\eta = 1$. This expression makes it clear that other choices of learning rates are possible. One could also utilize optimizers other than SGD on the clients, or use an alternative update rule on the server to apply the "pseudo-gradient". This family of algorithms, which we refer to collectively as FEDOPT, is formalized in Algorithm 1.

Here, CLIENTOPT and SERVEROPT are *gradient-based* optimizers with learning rates η_l and η respectively. Intuitively, CLIENTOPT aims to optimize the objective based on their local data while SERVEROPT optimizes it from a global perspective. FEDOPT naturally allows the use of adaptive optimizers (eg. ADAM, YOGI, etc.), as well as techniques such as server-side momentum (FEDAVGM) (Hsu et al., 2019). In its most general form, FEDOPT uses a CLIENTOPT whose updates can depend on globally aggregated statistics (e.g. server updates in the previous iterations). Also, we allow η and η_l to depend on the round t in order to encompass learning rate schedules. As we shall see, our theoretical and empirical analysis suggest that one should decay the client learning rate.

While FEDOPT has intuitive benefits over FEDAVG, it also raises a fundamental question: *Can the negative of the average model difference Δ_t be used as a pseudo-gradient in general server optimizer updates?* In this paper, we provide an affirmative answer to this question by establishing a theoretical basis for FEDOPT. More specifically, we develop principled adaptive optimizers for FL based on this framework and study their convergence behavior.

Algorithm 1 FEDOPT

1: Input: x_0, CLIENTOPT, SERVEROPT
2: **for** $t = 0, \cdots, T - 1$ **do**
3:     Sample a subset $\mathcal{S}$ of clients
4:     $x_{i,0}^t = x_t$
5:     **for** each client $i \in \mathcal{S}$ **in parallel do**
6:         **for** $k = 0, \cdots, K - 1$ **do**
7:             Compute an unbiased estimate $g_{i,k}^t$ of $\nabla F_i(x_{i,k}^t)$
8:             $x_{i,k+1}^t = \text{CLIENTOPT}(x_{i,k}^t, g_{i,k}^t, \eta_l, t)$
9:         $\Delta_i^t = x_{i,K}^t - x_t$
10:     $\Delta_t = \frac{1}{|\mathcal{S}|} \sum_{i \in \mathcal{S}} \Delta_i^t$
11:     $x_{t+1} = \text{SERVEROPT}(x_t, -\Delta_t, \eta, t)$

3 Adaptive Federated Optimization

In this section, we specialize FEDOPT to settings where SERVEROPT is an adaptive optimization method (one of ADAGRAD, YOGI or ADAM) and CLIENTOPT is SGD. Algorithm 2 provides pseudo-code for these adaptive federated optimizers. For simplicity, Algorithm 2 is stated without momentum, which is typically used in ADAM and YOGI. The parameter τ in all the algorithms controls their *degree of adaptivity*, with smaller values of τ representing higher degrees of adaptivity. We note that the updates of these methods are invariant to fixed multiplicative changes to the client learning rate η_l for appropriately chosen τ; although, as we shall see shortly, we still require η_l to be small enough.

We provide convergence analysis of these algorithms in the general nonconvex setting, assuming *full participation*, i.e. $\mathcal{S} = [m]$. However, our analysis can be extended to federated learning with *limited participation*. Furthermore, non-uniform weighted averaging typically used in FEDAVG (see (McMahan et al., 2017)) can also be incorporated into our analysis fairly easily.

Theorem 1. *Let Assumptions 1 to 3 hold, and let L, G, σ_l, σ_g be as defined therein. Let $\sigma^2 = \sigma_l^2 + 6K\sigma_g^2$. Consider the following conditions for η_l. (Condition I): $\eta_l \leq \frac{1}{8LK}$ and (Condition II):*

$$\eta_l \leq \frac{1}{3K} \min \left\{ \frac{1}{T^{1/10}} \left[\frac{\tau^3}{L^2 G^3} \right]^{1/5}, \frac{1}{T^{1/8}} \left[\frac{\tau^2}{L^3 G \eta} \right]^{1/4} \right\}.$$

Under Condition I only, the iterates of Algorithm 2 for FEDADAGRAD satisfy

$$\min_{0 \leq t \leq T-1} \mathbb{E} \|\nabla f(x_t)\|^2 \leq \mathcal{O} \left(\left[\frac{G}{\sqrt{T}} + \frac{\tau}{\eta_l K T} \right] (\Psi + \Psi_{var}) \right).$$

When both Condition I & II are satisfied,

$$\min_{0 \leq t \leq T-1} \mathbb{E} \|\nabla f(x_t)\|^2 \leq \mathcal{O} \left(\left[\frac{G}{\sqrt{T}} + \frac{\tau}{\eta_l K T} \right] \left(\Psi + \widetilde{\Psi}_{var} \right) \right).$$

Here, Ψ, Ψ_{var} and $\widetilde{\Psi}_{var}$ are defined as:

$$\Psi = \frac{f(x_0) - f(x^*)}{\eta} + \frac{5\eta_l^3 K^2 L^2 T}{2\tau} \sigma^2,$$

$$\Psi_{\text{var}} = \frac{d(\eta_l K G^2 + \tau \eta L)}{\tau} \left[1 + \log \left(1 + \frac{\eta_l^2 K^2 G^2 T}{\tau^2} \right) \right],$$

$$\widetilde{\Psi}_{\text{var}} = \frac{2\eta_l K G^2 + \tau \eta L}{\tau^2} \left[\frac{2\eta_l^2 K T}{m} \sigma_l^2 + 10\eta_l^4 K^3 L^2 T \sigma^2 \right].$$

All proofs are given in Appendix A. When η_l satisfies the condition in the second part the above result, we obtain a convergence rate depending on $\min\{\Psi_{\text{var}}, \widetilde{\Psi}_{\text{var}}\}$. To obtain an explicit dependence on T and K, we simplify the above result for a specific choice of η, η_l and τ.

4

Algorithm 2 FEDADAGRAD , FEDYOGI , and FEDADAM

1: Initialization: $x_0, v_{-1} \geq \tau^2$, optional decay $\beta_2 \in (0,1)$ for FEDYOGI and FEDADAM
2: **for** $t = 0, \cdots, T-1$ **do**
3:     Sample subset $\mathcal{S}$ of clients
4:     $x_{i,0}^t = x_t$
5:     **for** each client $i \in \mathcal{S}$ **in parallel do**
6:         **for** $k = 0, \cdots, K-1$ **do**
7:             Compute an unbiased estimate $g_{i,k}^t$ of $\nabla F_i(x_{i,k}^t)$
8:             $x_{i,k+1}^t = x_{i,k}^t - \eta_l g_{i,k}^t$
9:         $\Delta_i^t = x_{i,K}^t - x_t$
10:     $\Delta_t = \frac{1}{|\mathcal{S}|} \sum_{i \in \mathcal{S}} \Delta_i^t$
11:     $v_t = v_{t-1} + \Delta_t^2$ **(FEDADAGRAD)**
12:     $v_t = v_{t-1} - (1-\beta_2)\Delta_t^2 \,\mathrm{sign}(v_{t-1} - \Delta_t^2)$ **(FEDYOGI)**
13:     $v_t = \beta_2 v_{t-1} + (1-\beta_2)\Delta_t^2$ **(FEDADAM)**
14:     $x_{t+1} = x_t + \eta \frac{\Delta_t}{\sqrt{v_t}+\tau}$

Corollary 1. *Suppose η_l is such that the conditions in Theorem 1 are satisfied and $\eta_l = \Theta(1/(KL\sqrt{T}))$. Also suppose $\eta = \Theta(\sqrt{Km})$ and $\tau = G/L$. Then, for sufficiently large T, the iterates of Algorithm 2 for FEDADAGRAD satisfy*

$$\min_{0 \leq t \leq T-1} \mathbb{E}\|\nabla f(x_t)\|^2 = \mathcal{O}\left(\frac{f(x_0) - f(x^*)}{\sqrt{mKT}} + \frac{2\sigma_l^2 L}{G^2\sqrt{mKT}} + \frac{\sigma^2}{GKT} + \frac{\sigma^2 L\sqrt{m}}{G^2\sqrt{K}T^{3/2}} \right).$$

We defer a detailed discussion about our analysis and its implication to the end of the section.

Analysis of FEDADAM   Next, we provide the convergence analysis of FEDADAM. The proof of FEDYOGI is very similar and hence, we omit the details of FEDYOGI's analysis in the paper.

Theorem 2. *Let Assumptions 1 to 3 hold, and L, G, σ_l, σ_g be as defined therein. Let $\sigma^2 = \sigma_l^2 + 6K\sigma_g^2$. Suppose the client learning rate satisfies $\eta_l \leq \frac{1}{8LK}$ and*

$$\eta_l \leq \frac{1}{6K} \min\left\{ \left[\frac{\tau}{GL}\right]^{1/2}, \left[\frac{\tau^2}{GL^3\eta}\right]^{1/4} \right\}.$$

Then the iterates of Algorithm 2 for FEDADAM satisfy

$$\min_{0 \leq t \leq T-1} \mathbb{E}\|\nabla f(x_t)\|^2 = \mathcal{O}\left(\frac{\sqrt{\beta_2}\eta_l KG + \tau}{\eta_l KT} \left(\Psi + \Psi_{\mathrm{var}}\right) \right)$$

where

$$\Psi = \frac{f(x_0) - f(x^*)}{\eta} + \frac{5\eta_l^3 K^2 L^2 T}{2\tau}\sigma^2, \quad \Psi_{var} = \left(G + \frac{\eta L}{2}\right)\left[\frac{4\eta_l^2 KT}{m\tau^2}\sigma_l^2 + \frac{20\eta_l^4 K^3 L^2 T}{\tau^2}\sigma^2\right].$$

Similar to the FEDADAGRAD case, we restate the above result for a specific choice of η_l, η and τ in order to highlight the dependence of K and T.

Corollary 2. *Suppose η_l is chosen such that the conditions in Theorem 2 are satisfied and that $\eta_l = \Theta(1/(KL\sqrt{T}))$. Also, suppose $\eta = \Theta(\sqrt{Km})$ and $\tau = G/L$. Then, for sufficiently large T, the iterates of Algorithm 2 for FEDADAM satisfy*

$$\min_{0 \leq t \leq T-1} \mathbb{E}\|\nabla f(x_t)\|^2 = \mathcal{O}\left(\frac{f(x_0) - f(x^*)}{\sqrt{mKT}} + \frac{2\sigma_l^2 L}{G^2\sqrt{mKT}} + \frac{\sigma^2}{GKT} + \frac{\sigma^2 L\sqrt{m}}{G^2\sqrt{K}T^{3/2}} \right).$$

Discussion We briefly discuss our theoretical analysis and its implications in the FL setting. The convergence rates for FEDADAGRAD and FEDADAM are similar, so our discussion applies to all the adaptive federated optimization algorithms (including FEDYOGI) proposed in the paper.

(i) **Comparison of convergence rates.** When T is sufficiently large compared to K, $\mathcal{O}(1/\sqrt{mKT})$ is the dominant term in Corollary 1 & 2. Thus, we effectively obtain a convergence rate of $\mathcal{O}(1/\sqrt{mKT})$, which matches the *best known rate* for the general non-convex setting of our interest (e.g. see (Karimireddy et al., 2019)). We also note that in the *i.i.d* setting considered in (Wang and Joshi, 2018), which corresponds to $\sigma_g = 0$, we match their convergence rates. Similar to the centralized setting, it is possible to obtain convergence rates with better dependence on constants for federated adaptive methods, compared to FEDAVG, by incorporating non-uniform bounds on gradients across coordinates (Zaheer et al., 2018).

(ii) **Learning rates & their decay.** Note that the client learning rate of $1/\sqrt{T}$ in our convergence analysis requires knowledge of the number of rounds T beforehand; however, it is easy to generalize our analysis to the case where η_l is decayed at a rate of $1/\sqrt{t}$. Observe that one must decay the client learning rate, not the server learning rate, to obtain convergence. This is due to the fact that the *client drift* introduced by the local updates does not vanish as $T \to \infty$ when η_l is not decayed. As we show later in our empirical analysis, learning rate decay can greatly improve performance. Also, note the inverse relationship between the client and server learning rates, η_l and η, in Corollary 1 & 2, which we also observe in our empirical analysis (Figure 2).

(iii) **Communication efficiency & local steps.** The total communication cost of the algorithms depends on the number of communication rounds T. From Corollary 1 & 2, it is clear that a larger K leads to fewer rounds of communication as long as $K = \mathcal{O}(T\sigma_l^2/\sigma_g^2)$. Thus, the number of local iterations can be large when either the ratio σ_l^2/σ_g^2 or T is large. In the extreme *i.i.d* setting where $\sigma_g = 0$, unsurprisingly, K can be very large.

As mentioned earlier, for the sake of simplicity, our analysis assumes full-participation i.e., $\mathcal{S} = [m]$. However, our analysis can be easily generalized to the case of limited participation at the cost of an additional variance term in the convergence rates that depends on the cardinality of the subset $\mathcal{S}$.

4   Experimental Evaluation: Datasets, Tasks, and Methods

We present an empirical evaluation of the federated optimization algorithms introduced in Sections 2 and 3 on what we believe is the most extensive and representative suite of federated datasets and modeling tasks that has been presented to date. Our goal, in addition to validating our theoretical results, is to understand how the use of adaptive server optimizers, momentum, and learning rate decay can help improve convergence, particularly with respect to the defacto standard of FEDAVG. To accomplish this, we conduct extensive simulations of federated learning on six diverse and representative learning tasks across four datasets. Notably, three of the four datasets use a naturally-arising client partitioning, highly representative of real-world federated learning problems.

Datasets, models, and tasks We perform six tasks on four datasets: CIFAR-100 (Krizhevsky and Hinton, 2009), EMNIST (Cohen et al., 2017), Shakespeare (McMahan et al., 2017), and Stack Overflow (Authors, 2019). The first two are image datasets, the last two are text datasets. For CIFAR-100, we train ResNet-18 (replacing batch norm with group norm (Hsieh et al., 2019)). For EMNIST, we train a CNN to do character recognition (EMNIST CR) and a bottleneck autoencoder (EMNIST AE). For Shakespeare, we train an RNN for next-character-prediction. For Stack Overflow, we perform tag prediction using logistic regression on bag-of-words vectors (SO LR) and train an RNN to do next-word-prediction (SO NWP). All datasets are partitioned into training and test sets, each with their own set of clients. Statistics on the number of clients and examples in both the training and test splits of the datasets are given in Table 1. For full details on the datasets, see Appendix C.

Implementation We implement all algorithms in TensorFlow Federated (Ingerman and Ostrowski, 2019). We provide an open-source implementation of our optimizers and all experiments in this work.[2] In all experiments, client sampling is done uniformly at random from all training clients, without replacement within a given round, but with replacement across rounds. There are two important practical points about our implementation. First, rather than using a constant

---

[2]https://github.com/tensorflow/federated/tree/master/tensorflow_federated/python/research/optimization

Table 1: Dataset statistics.

DATASET	TRAIN CLIENTS	TRAIN EXAMPLES	TEST CLIENTS	TEST EXAMPLES
CIFAR-100	500	50,000	100	10,000
EMNIST-62	3,400	671,585	3,400	77,483
SHAKESPEARE	715	16,068	715	2,356
STACKOVERFLOW	342,477	135,818,730	204,088	16,586,035

K local steps per client, we do E *client epochs* of training over each client's local dataset at each round. Second, in order to account for the varying number of gradient steps per client, we take a weighted average of the client outputs Δ_i^t according to the number of training samples of the client. While this is not used in our theoretical analysis, this follows the approach of (McMahan et al., 2017), which has been shown to often outperform uniform weighting. For a full description of the algorithms used, see Appendix B.

Optimizers and hyperparameter tuning In our experiments, we compare FEDADAGRAD, FEDADAM, and FEDYOGI to the special case of FEDOPT where CLIENTOPT and SERVEROPT are SGD with tuned learning rates of η_l and η. We use no momentum on the client, and a momentum parameter of either 0 or 0.9 on the server. In a slight abuse of notation, we refer to the former as FEDAVG and the latter as FEDAVGM. We select η_l, η, and τ by grid-search tuning (see Appendix D.2). For FEDADAM and FEDYOGI, we fix a momentum parameter of $\beta_1 = 0.9$ and a second moment parameter of $\beta_2 = 0.99$. For Stack Overflow NWP, we sample 50 clients per round, for all other tasks we sample 10. For further details on hyperparameters, tuning, and the best-performing hyperparameters, see Appendix D.

Given the large number of hyperparameters to tune, and to avoid conflating variables, we fix the batch size at a per-task level. When comparing centralized training to federated training in Section 5, we use the same batch size in both federated and centralized training. A full summary of the batch sizes is given in Table 2.

Table 2: Batch sizes used for each task.

TASK	BATCH SIZE
CIFAR-100	20
EMNIST AE	20
EMNIST CR	20
SHAKESPEARE	4
STACKOVERFLOW LR	100
STACKOVERFLOW NWP	16

5 Experimental Evaluation: Results

In this section, we compare the performance of our adaptive methods to FEDAVG and FEDAVGM on the tasks described above. For all tasks, we measure the performance on a validation set throughout training. Since all algorithms exchange equal-sized objects between server and clients, we use the number of communication rounds as a proxy for wall-clock training time. We use the full test set for all tasks except Stack Overflow tasks, for which we use 10,000 randomly sampled test examples (due to the size of the test dataset), and measure the performance on the full test set at the end of training.

5.1 Constant learning rate

We investigate whether adaptive optimization with tuned but constant η_l and η is enough to outperform FEDAVG. We run each optimizer with $E = 1$ local client epochs, and select η_l and η based on the average validation performance over the last 100 communication rounds (see Appendix D for the learning rate grids and the best learning rates). A plot of the validation accuracy is given in Figure 1, and Table 3 summarizes the last-100-round validation performance.

As discussed in Section 4, we use a subsampled version of the test dataset as the validation set, due to the prohibitively large number of clients and examples in Stack Overflow. The validation set consists of 10,000 randomly selected examples from the test set. However, once training is completed, we also evaluate on the full test dataset. The full test set performance for Stack Overflow is given in Table 4 and shows similar results to Table Table 3. We discuss salient features of both tables below.

Table 3: Average validation performance over the last 100 rounds: % accuracy for rows 1–4; Recall@5 for StackOverflow LR; and MSE for EMNIST AE. Performance within $0.5\%/0.05/0.25$ of the best result are shown in bold.

FED...	ADAGRAD	ADAM	YOGI	AVGM	AVG
CIFAR-100	47.2	**52.3**	**52.3**	50.6	39.1
EMNIST CR	**85.3**	**85.5**	**85.6**	**85.6**	84.8
SHAKESPEARE	**57.6**	57.2	**57.3**	**57.3**	57.0
STACK OV... NWP	19.0	**23.4**	**23.5**	21.0	15.6
STACK OV... LR	**0.68**	**0.66**	**0.66**	0.36	0.28
EMNIST AE	7.21	16.8	**0.98**	**1.20**	2.60

Table 4: Test set performance for Stack Overflow tasks after training: Accuracy for NWP and Recall@5 for LR. Performance within within $0.5\%/0.05$ of the best result are shown in bold.

FED...	ADAGRAD	ADAM	YOGI	AVGM	AVG
STACK OVERFLOW NWP	20.3	**24.3**	**24.4**	22.3	17.3
STACK OVERFLOW LR	**0.66**	0.64	0.64	0.32	0.33

Sparse-gradient tasks Text data naturally produces long-tailed feature distributions, often leading to approximately-sparse gradients which adaptive optimizers can capitalize on. This has been observed many times for centralized training, and we show this also applies to FL. Both Stack Overflow tasks exhibit such behavior, though we emphasize that these two tasks are otherwise dramatically different—in feature representation (bag-of-words vs. variable-length token sequence), model architecture (GLM vs deep network), and optimization landscape (convex vs non-convex).

In both tasks, words that do not appear in a client's set of examples will produce zero (for LR) or near-zero (for NWP, due to the softmax) client updates. Thus, the accumulator $v_{t,j}$ in Algorithm 2 will remain small for parameters tied to rare words, allowing large updates to be made when they do occur; conversely, $v_{t,j}$ will grow quickly for common words, preventing the parameter pertaining to those words from oscillating. This intuition is born out of Figure 1, where adaptive optimizers dramatically outperform non-adaptive methods. For the non-convex NWP task, momentum also appears to be critical, whereas it slightly hinders performance for the convex LR task.

Dense-gradient tasks The results for CIFAR-100, EMNIST AE/CR and Shakespeare are also given in Figure 1. These tasks lack the sparse-gradient structure of the two previous tasks (see Appendix C for architecture and featurization details). For EMNIST AE, we normalize the MSE by the output dimension 28×28 throughout. Two of the tasks, EMNIST CR and Shakespeare, are relatively easy—all optimizers perform well *once suitably tuned*. For CIFAR-100
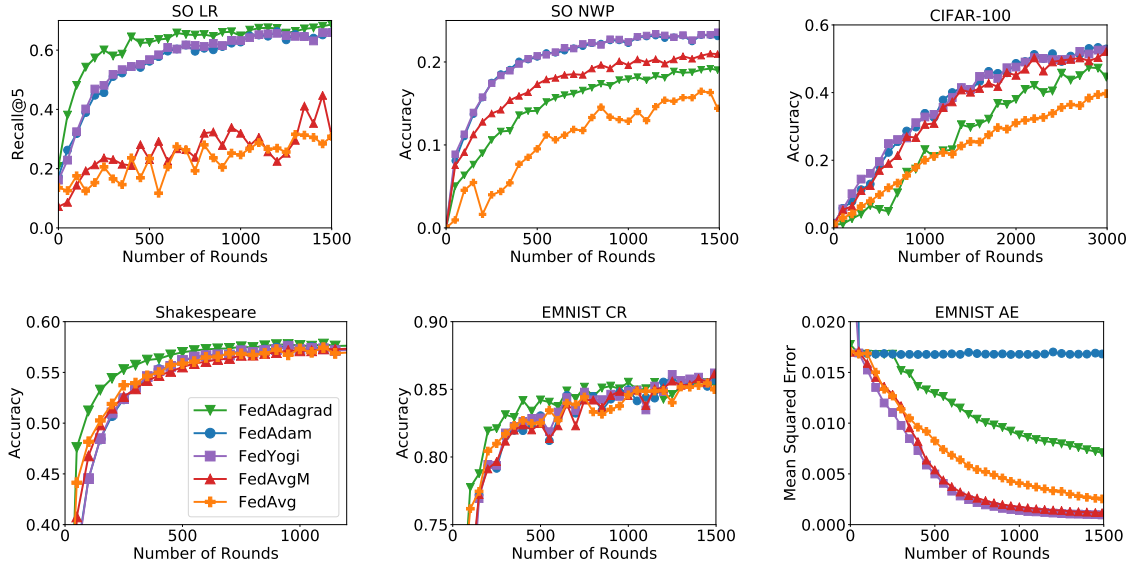
Figure 1: Validation set performance using constant learning rates η and η_l tuned to achieve the best performance on the last 100 communication rounds; see Appendix D.2 for grids.

and EMNIST AE, we see that adaptive server optimizers and momentum can offer a substantial improvement over FEDAVG. FEDYOGI was the only optimizer to perform well in all settings. FEDAVGM was slightly outperformed by FEDADAM and FEDYOGI on CIFAR-100, and FEDADAM failed to converge for any server/client learning rate combinations on EMNIST AE. We note that the bottleneck architecture used tends to create saddle points that can be difficult to escape (Zaheer et al., 2018).

5.2 On the ratio of client and server learning rate

By Theorem 1, we expect an inverse relationship between the client learning rate η_l and the best corresponding server learning rate η. Intuitively, if the clients learning rate is large, the server must account for drift by reducing its learning rate. To validate this, we plot the optimal server learning rate for each client learning rate in Figure 2.

We see that in most tasks, save for EMNIST AE, there is a clear inverse relationship between the client learning rate and the best corresponding server learning rate. This is intuitively clear: If the client is using a small learning rate, then the server must compensate with a larger learning rate in order to make sufficient progress. Conversely, if the client is using a large learning rate, then it stands to fit much more to its own local dataset. However, since clients may have different datasets, this can result in *client drift* (Karimireddy et al., 2019), which can mar convergence. Thus, the server must compensate with a smaller learning rate. This trend is especially pronounced for FEDYOGI and FEDAVGM (though when the client learning rate is too small or too large, training instability can violate this trend).

For EMNIST AE, we see a less clear relation. This is partially to be expected. As shown by Zaheer et al. (2018), the primary obstacle in EMNIST AE is escaping saddle points. However, Theorem 1 concerns convergence to a critical point, not how to escape saddle points. This may involve a more nuanced relation between client and server learning rates. This is an important area of study (see work by Jin et al. (2017) and Reddi et al. (2017), for example), and one in which adaptive optimizers have found great success (Staib et al., 2019). However, this is beyond the scope of our work, and we leave a more detailed analysis of escaping saddle points using adaptive federated optimization to future work.
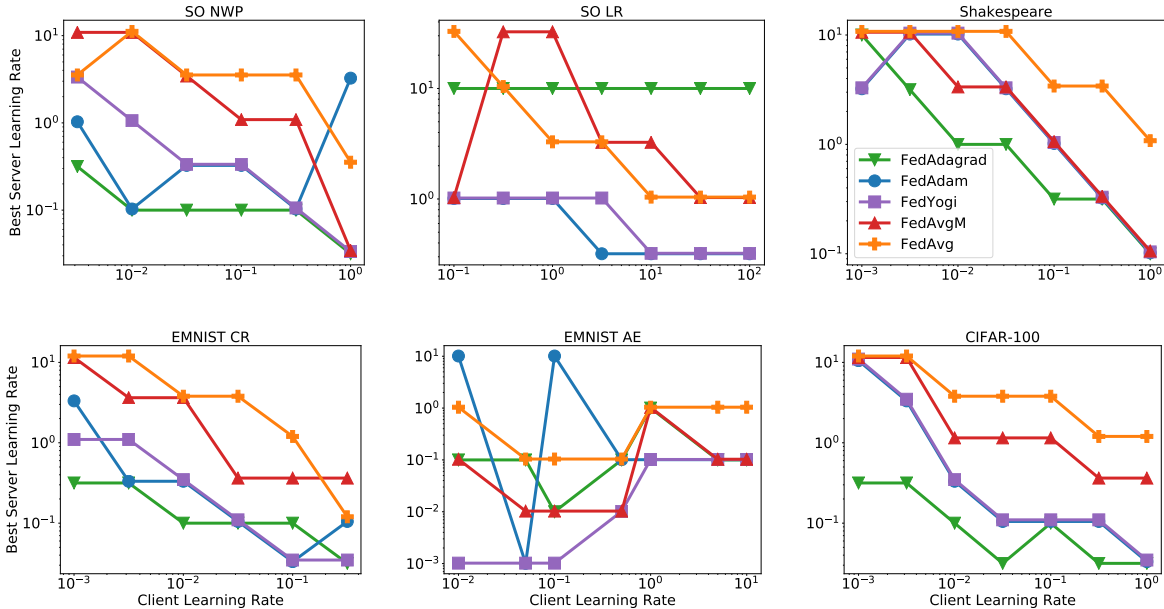
Figure 2: The best server learning rate in our hyperparameter tuning grids for each client learning rate, optimizers, and task. We select the server learning rates based on the average performance over the last 100 communication rounds.

5.3 Learning rate decay

Despite the success of adaptive methods, it is natural to ask if there is still more to be gained. To test this, we trained the EMNIST CR model in a centralized fashion on a shuffled version of the dataset. We trained for 100 epochs and used tuned learning rates for each (centralized) optimizer, achieving an accuracy of 88% (see Table 5, CENTRALIZED row), significantly above the best EMNIST CR results from Table 3. The theoretical results in Section 3 point to a partial explanation, as they only hold when the client learning rate is small (on the order of $1/\sqrt{T}$, where T is the total number of communication rounds) or the client learning rate is decayed over time.

Table 5: (Top) Test accuracy (%) of a model trained centrally with various optimizers. (Bottom) Average test accuracy (%) over the last 100 rounds of various federated optimizers on the EMNIST CR task, using three schedules for η_l. Accuracies within 0.5% of the best result are shown in bold.

	ADAGRAD	ADAM	YOGI	SGDM	SGD
CENTRALIZED	88.0	87.9	88.0	87.7	87.7

FED...	ADAGRAD	ADAM	YOGI	AVGM	AVG
CONSTANT η_l	85.3	85.5	85.6	85.6	84.8
INVSQRT	84.3	86.2	85.7	85.7	84.4
EXPDECAY	85.5	**86.8**	**86.8**	**86.4**	**86.7**

To validate this, we use two client learning rate schedules, INVSQRT (an inverse square root decay of $\eta_l/\sqrt{t}$) and EXPDECAY (a "staircase" exponential decay schedule where η_l is decreased by a factor of 0.1 every 500 rounds (Goyal et al., 2017)). We use $E = 10$ client epochs, and sample 10 clients per round. Table 5 gives the results. EXPDECAY improves the accuracy of all optimizers, and allows most to get close to the best centralized accuracy. We find particular efficacy in using the EXPDECAY learning rate schedule to compensate for deficiencies of vanilla FedAvg.

10

We also compare the performance of adaptive optimizers (using ExpDecay) with vanilla FedAvg (without ExpDecay). For FedAvg, we vary the number of local client epochs E over $\{1, 5, 10\}$, while we use 10 local client epochs for the adaptive optimizers. We apply these methods to the EMNIST CR task. In all cases, we use 10 clients per round. We also compare to the best centralized accuracy in Table 5. The results are in Figure 3.
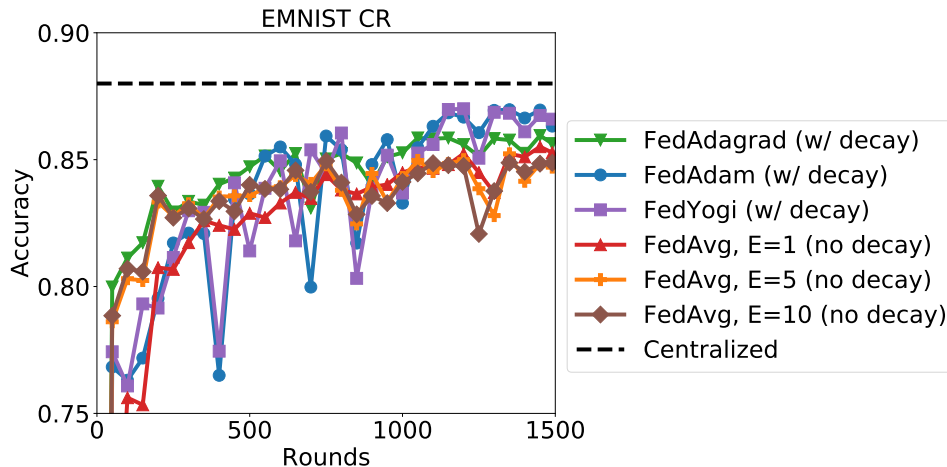

Figure 3: The validation accuracy over time of various optimizers on EMNIST CR, as well as the best centralized accuracy.

While FedAvg with $E = 10$ achieved good performance initially, it obtained slightly worse accuracy than $E \in \{1, 5\}$ after enough rounds. On the other hand, the adaptive optimizers with ExpDecay surpass all three versions of FedAvg after the second client learning rate decay occurs, and only perform better thereafter.

6 Conclusion

In this paper, we demonstrated that adaptive optimizers can be powerful tools in improving the convergence of federated learning. Moreover, we showed that by using a simple client/server optimizer framework, we can apply adaptive optimizers to federated learning in a principled and intuitive manner. While our work establishes the theoretical and empirical benefits of this framework, it also raises many interesting questions about how best to perform federated optimization. Example directions for future research include exploring the use of momentum or adaptive client optimizers and developing comprehensive heuristics for setting learning rates and other hyperparameters.

References

The TensorFlow Federated Authors. TensorFlow Federated Stack Overflow dataset, 2019. URL https://www.tensorflow.org/federated/api_docs/python/tff/simulation/datasets/stackoverflow/load_data.

Debraj Basu, Deepesh Data, Can Karakus, and Suhas Diggavi. Qsparse-local-SGD: Distributed SGD with quantization, sparsification and local computations. In *Advances in Neural Information Processing Systems*, pages 14668–14679, 2019.

Sebastian Caldas, Peter Wu, Tian Li, Jakub Konečný, H Brendan McMahan, Virginia Smith, and Ameet Talwalkar. LEAF: A benchmark for federated settings. *arXiv preprint arXiv:1812.01097*, 2018.

Gregory Cohen, Saeed Afshar, Jonathan Tapson, and Andre Van Schaik. EMNIST: Extending MNIST to handwritten letters. In *2017 International Joint Conference on Neural Networks (IJCNN)*, pages 2921–2926. IEEE, 2017.

John Duchi, Elad Hazan, and Yoram Singer. Adaptive subgradient methods for online learning and stochastic optimization. *Journal of Machine Learning Research*, 12(Jul):2121–2159, 2011.

Priya Goyal, Piotr Dollár, Ross Girshick, Pieter Noordhuis, Lukasz Wesolowski, Aapo Kyrola, Andrew Tulloch, Yangqing Jia, and Kaiming He. Accurate, large minibatch SGD: Training ImageNet in 1 hour. *arXiv preprint arXiv:1706.02677*, 2017.

Kevin Hsieh, Amar Phanishayee, Onur Mutlu, and Phillip B Gibbons. The non-IID data quagmire of decentralized machine learning. *arXiv preprint arXiv:1910.00189*, 2019.

Tzu-Ming Harry Hsu, Hang Qi, and Matthew Brown. Measuring the effects of non-identical data distribution for federated visual classification. *arXiv preprint arXiv:1909.06335*, 2019.

Alex Ingerman and Krzys Ostrowski. Introducing TensorFlow Federated, 2019. URL https://medium.com/tensorflow/introducing-tensorflow-federated-a4147aa20041.

Chi Jin, Rong Ge, Praneeth Netrapalli, Sham M Kakade, and Michael I Jordan. How to escape saddle points efficiently. *arXiv preprint arXiv:1703.00887*, 2017.

Peter Kairouz, H Brendan McMahan, Brendan Avent, Aurélien Bellet, Mehdi Bennis, Arjun Nitin Bhagoji, Keith Bonawitz, Zachary Charles, Graham Cormode, Rachel Cummings, et al. Advances and open problems in federated learning. *arXiv preprint arXiv:1912.04977*, 2019.

Sai Praneeth Karimireddy, Satyen Kale, Mehryar Mohri, Sashank J Reddi, Sebastian U Stich, and Ananda Theertha Suresh. SCAFFOLD: Stochastic controlled averaging for on-device federated learning. *arXiv preprint arXiv:1910.06378*, 2019.

Ahmed Khaled, Konstantin Mishchenko, and Peter Richtárik. First analysis of local GD on heterogeneous data. *arXiv preprint arXiv:1909.04715*, 2019.

Diederik P. Kingma and Jimmy Ba. Adam: A method for stochastic optimization. In *3rd International Conference on Learning Representations, ICLR 2015, San Diego, CA, USA, May 7-9, 2015, Conference Track Proceedings*, 2015.

Alex Krizhevsky and Geoffrey Hinton. Learning multiple layers of features from tiny images. Technical report, Citeseer, 2009.

Tian Li, Anit Kumar Sahu, Manzil Zaheer, Maziar Sanjabi, Ameet Talwalkar, and Virginia Smith. Federated optimization in heterogeneous networks. *arXiv preprint arXiv:1812.06127*, 2018.

Tian Li, Anit Kumar Sahu, Ameet Talwalkar, and Virginia Smith. Federated learning: Challenges, methods, and future directions. *arXiv preprint arXiv:1908.07873*, 2019a.

Wei Li and Andrew McCallum. Pachinko allocation: DAG-structured mixture models of topic correlations. In *Proceedings of the 23rd international conference on Machine learning*, pages 577–584, 2006.

Xiang Li, Kaixuan Huang, Wenhao Yang, Shusen Wang, and Zhihua Zhang. On the convergence of FedAvg on non-IID data. *arXiv preprint arXiv:1907.02189*, 2019b.

Xiaoyu Li and Francesco Orabona. On the convergence of stochastic gradient descent with adaptive stepsizes. *arXiv preprint arXiv:1805.08114*, 2018.

Brendan McMahan, Eider Moore, Daniel Ramage, Seth Hampson, and Blaise Agüera y Arcas. Communication-efficient learning of deep networks from decentralized data. In *Proceedings of the 20th International Conference on Artificial Intelligence and Statistics, AISTATS 2017, 20-22 April 2017, Fort Lauderdale, FL, USA*, pages 1273–1282, 2017. URL http://proceedings.mlr.press/v54/mcmahan17a.html.

H. Brendan McMahan and Matthew J. Streeter. Adaptive bound optimization for online convex optimization. In *COLT The 23rd Conference on Learning Theory*, 2010.

Sashank J Reddi, Ahmed Hefny, Suvrit Sra, Barnabás Póczós, and Alex Smola. Stochastic variance reduction for nonconvex optimization. *arXiv:1603.06160*, 2016.

Sashank J Reddi, Manzil Zaheer, Suvrit Sra, Barnabas Poczos, Francis Bach, Ruslan Salakhutdinov, and Alexander J Smola. A generic approach for escaping saddle points. *arXiv preprint arXiv:1709.01434*, 2017.

Matthew Staib, Sashank J Reddi, Satyen Kale, Sanjiv Kumar, and Suvrit Sra. Escaping saddle points with adaptive gradient methods. *arXiv preprint arXiv:1901.09149*, 2019.

Sebastian U. Stich. Local SGD converges fast and communicates little. In *International Conference on Learning Representations*, 2019. URL https://openreview.net/forum?id=S1g2JnRcFX.

Sebastian U Stich and Sai Praneeth Karimireddy. The error-feedback framework: Better rates for SGD with delayed gradients and compressed communication. *arXiv preprint arXiv:1909.05350*, 2019.

Jianyu Wang and Gauri Joshi. Cooperative SGD: A unified framework for the design and analysis of communication-efficient SGD algorithms. *arXiv preprint arXiv:1808.07576*, 2018.

Shiqiang Wang, Tiffany Tuor, Theodoros Salonidis, Kin K Leung, Christian Makaya, Ting He, and Kevin Chan. Adaptive federated learning in resource constrained edge computing systems. *IEEE Journal on Selected Areas in Communications*, 37(6):1205–1221, 2019.

Rachel Ward, Xiaoxia Wu, and Leon Bottou. Adagrad stepsizes: Sharp convergence over nonconvex landscapes, from any initialization. *arXiv preprint arXiv:1806.01811*, 2018.

Xiaoxia Wu, Simon S Du, and Rachel Ward. Global convergence of adaptive gradient methods for an over-parameterized neural network. *arXiv preprint arXiv:1902.07111*, 2019.

Yuxin Wu and Kaiming He. Group normalization. In *Proceedings of the European Conference on Computer Vision (ECCV)*, pages 3–19, 2018.

Cong Xie, Oluwasanmi Koyejo, Indranil Gupta, and Haibin Lin. Local AdaAlter: Communication-efficient stochastic gradient descent with adaptive learning rates. *arXiv preprint arXiv:1911.09030*, 2019.

Hao Yu, Sen Yang, and Shenghuo Zhu. Parallel restarted SGD with faster convergence and less communication: Demystifying why model averaging works for deep learning. In *Proceedings of the AAAI Conference on Artificial Intelligence*, volume 33, pages 5693–5700, 2019.

Manzil Zaheer, Sashank Reddi, Devendra Sachan, Satyen Kale, and Sanjiv Kumar. Adaptive methods for nonconvex optimization. In *Advances in Neural Information Processing Systems*, pages 9815–9825, 2018.

Jingzhao Zhang, Sai Praneeth Karimireddy, Andreas Veit, Seungyeon Kim, Sashank J. Reddi, Sanjiv Kumar, and Suvrit Sra. Why ADAM beats SGD for attention models. *arXiv preprint arxiv:1912.03194*, 2019.

Martin Zinkevich, Markus Weimer, Lihong Li, and Alex J Smola. Parallelized stochastic gradient descent. In *Advances in neural information processing systems*, pages 2595–2603, 2010.

A   Proof of results

A.1   Theorem 1

Proof of Theorem 1. Recall that the server update of FEDADAGRAD is the following

$$x_{t+1,i} = x_{t,i} + \eta \frac{\Delta_{t,i}}{\sqrt{v_{t,i}} + \tau},$$

for all $i \in [d]$. Since the function f is L-smooth, we have the following:

$$f(x_{t+1}) \le f(x_t) + \langle \nabla f(x_t), x_{t+1} - x_t \rangle + \frac{L}{2} \|x_{t+1} - x_t\|^2$$

$$= f(x_t) + \eta \left\langle \nabla f(x_t), \frac{\Delta_t}{\sqrt{v_t} + \tau} \right\rangle + \frac{\eta^2 L}{2} \sum_{i=1}^{d} \frac{\Delta_{t,i}^2}{\left(\sqrt{v_{t,i}} + \tau\right)^2} \tag{2}$$

The second step follows simply from FEDADAGRAD's update. We take the expectation of $f(x_{t+1})$ (over randomness at time step t) in the above inequality:

$$\mathbb{E}_t[f(x_{t+1})] \le f(x_t) + \eta \left\langle \nabla f(x_t), \mathbb{E}_t \left[\frac{\Delta_t}{\sqrt{v_t} + \tau} \right] \right\rangle + \frac{\eta^2 L}{2} \sum_{i=1}^{d} \mathbb{E}_t \left[\frac{\Delta_{t,i}^2}{\left(\sqrt{v_{t,i}} + \tau\right)^2} \right]$$

$$= f(x_t) + \eta \left\langle \nabla f(x_t), \mathbb{E}_t \left[\frac{\Delta_t}{\sqrt{v_t} + \tau} - \frac{\Delta_t}{\sqrt{v_{t-1}} + \tau} + \frac{\Delta_t}{\sqrt{v_{t-1}} + \tau} \right] \right\rangle$$

$$+ \frac{\eta^2 L}{2} \sum_{j=1}^{d} \mathbb{E}_t \left[\frac{\Delta_{t,j}^2}{\left(\sqrt{v_{t,j}} + \tau\right)^2} \right]$$

$$= f(x_t) + \eta \underbrace{\left\langle \nabla f(x_t), \mathbb{E}_t \left[\frac{\Delta_t}{\sqrt{v_{t-1}} + \tau} \right] \right\rangle}_{T_1} + \eta \underbrace{\left\langle \nabla f(x_t), \mathbb{E}_t \left[\frac{\Delta_t}{\sqrt{v_t} + \tau} - \frac{\Delta_t}{\sqrt{v_{t-1}} + \tau} \right] \right\rangle}_{T_2}$$

$$+ \frac{\eta^2 L}{2} \sum_{j=1}^{d} \mathbb{E}_t \left[\frac{\Delta_{t,j}^2}{\left(\sqrt{v_{t,j}} + \tau\right)^2} \right] \tag{3}$$

We will first bound T_2 in the following manner:

$$T_2 = \left\langle \nabla f(x_t), \mathbb{E}_t \left[\frac{\Delta_t}{\sqrt{v_t} + \tau} - \frac{\Delta_t}{\sqrt{v_{t-1}} + \tau} \right] \right\rangle$$

$$= \mathbb{E}_t \sum_{j=1}^{d} [\nabla f(x_t)]_j \times \left[\frac{\Delta_{t,j}}{\sqrt{v_{t,j}} + \tau} - \frac{\Delta_{t,j}}{\sqrt{v_{t-1,j}} + \tau} \right]$$

$$= \mathbb{E}_t \sum_{j=1}^{d} [\nabla f(x_t)]_j \times \Delta_{t,j} \times \left[\frac{\sqrt{v_{t-1,j}} - \sqrt{v_{t,j}}}{(\sqrt{v_{t,j}} + \tau)(\sqrt{v_{t-1,j}} + \tau)}, \right]$$

and recalling $v_t = v_{t-1} + \Delta_t^2$ so $-\Delta_{t,j}^2 = (\sqrt{v_{t-1,j}} - \sqrt{v_{t,j}})(\sqrt{v_{t-1,j}} + \sqrt{v_{t,j}})$ we have,

$$= \mathbb{E}_t \sum_{j=1}^{d} [\nabla f(x_t)]_j \times \Delta_{t,j} \times \left[\frac{-\Delta_{t,j}^2}{(\sqrt{v_{t,j}} + \tau)(\sqrt{v_{t-1,j}} + \tau)(\sqrt{v_{t-1,j}} + \sqrt{v_{t,j}})} \right]$$

$$\le \mathbb{E}_t \sum_{j=1}^{d} |\nabla f(x_t)]_j| \times |\Delta_{t,j}| \times \left[\frac{\Delta_{t,j}^2}{(\sqrt{v_{t,j}} + \tau)(\sqrt{v_{t-1,j}} + \tau)(\sqrt{v_{t-1,j}} + \sqrt{v_{t,j}})} \right]$$

$$\le \mathbb{E}_t \sum_{j=1}^{d} |\nabla f(x_t)]_j| \times |\Delta_{t,j}| \times \left[\frac{\Delta_{t,j}^2}{(v_{t,j} + \tau^2)(\sqrt{v_{t-1,j}} + \tau)} \right] \qquad \text{since } v_{t-1,j} \ge \tau^2.$$

Here $v_{t-1,j} \geq \tau$ since $v_{-1} \geq \tau$ (see the initialization of Algorithm 2) and $v_{t,j}$ is increasing in t. The above bound can be further upper bounded in the following manner:

$$T_2 \leq \mathbb{E}_t \sum_{j=1}^{d} \eta_l K G^2 \left[\frac{\Delta_{t,j}^2}{(v_{t,j} + \tau^2)(\sqrt{v_{t-1,j}} + \tau)} \right] \qquad \text{since } [\nabla f(x_t)]_i \leq G \text{ and } \Delta_{t,i} \leq \eta_l K G$$

$$\leq \mathbb{E}_t \sum_{j=1}^{d} \frac{\eta_l K G^2}{\tau} \left[\frac{\Delta_{t,j}^2}{\sum_{l=0}^{t} \Delta_{l,j}^2 + \tau^2} \right] \qquad \text{since } \sqrt{v_{t-1,j}} \geq 0. \qquad (4)$$

Bounding T_1 We now turn our attention to bounding the term T_1, which we need to be sufficiently negative. We observe the following:

$$T_1 = \left\langle \nabla f(x_t), \mathbb{E}_t \left[\frac{\Delta_t}{\sqrt{v_{t-1}} + \tau} \right] \right\rangle$$

$$= \left\langle \frac{\nabla f(x_t)}{\sqrt{v_{t-1}} + \tau}, \mathbb{E}_t \left[\Delta_t - \eta_l K \nabla f(x_t) + \eta_l K \nabla f(x_t) \right] \right\rangle$$

$$= -\eta_l K \sum_{j=1}^{d} \frac{[\nabla f(x_t)]_j^2}{\sqrt{v_{t-1,j}} + \tau} + \underbrace{\left\langle \frac{\nabla f(x_t)}{\sqrt{v_{t-1}} + \tau}, \mathbb{E}_t \left[\Delta_t + \eta_l K \nabla f(x_t) \right] \right\rangle}_{T_3}. \qquad (5)$$

In order to bound T_1, we use the following upper bound on T_3 (which captures the difference between the actual update Δ_t and an appropriate scaling of $-\nabla f(x_t)$):

$$T_3 = \left\langle \frac{\nabla f(x_t)}{\sqrt{v_{t-1}} + \tau}, \mathbb{E}_t \left[\Delta_t + \eta_l K \nabla f(x_t) \right] \right\rangle$$

$$= \left\langle \frac{\nabla f(x_t)}{\sqrt{v_{t-1}} + \tau}, \mathbb{E}_t \left[-\frac{1}{m} \sum_{i=1}^{m} \sum_{k=0}^{K-1} \eta_l g_{i,k}^t + \eta_l K \nabla f(x_t) \right] \right\rangle$$

$$= \left\langle \frac{\nabla f(x_t)}{\sqrt{v_{t-1}} + \tau}, \mathbb{E}_t \left[-\frac{1}{m} \sum_{i=1}^{m} \sum_{k=0}^{K-1} \eta_l \nabla F_i(x_{i,k}^t) + \eta_l K \nabla f(x_t) \right] \right\rangle.$$

Here we used the fact that $\nabla f(x_t) = \frac{1}{m} \sum_{i=1}^{m} \nabla F_i(x_t)$ and $g_{i,k}^t$ is an unbiased estimator of the gradient at $x_{i,k}^t$, we further bound T_3 as follows using a simple application of the fact that $ab \leq (a^2 + b^2)/2.$:

$$T_3 \leq \frac{\eta_l K}{2} \sum_{j=1}^{d} \frac{[\nabla f(x_t)]_j^2}{\sqrt{v_{t-1,j}} + \tau} + \frac{\eta_l}{2K} \mathbb{E}_t \left[\left\| \frac{1}{m} \sum_{i=1}^{m} \sum_{k=0}^{K-1} \frac{\nabla F_i(x_{i,k}^t)}{\sqrt{\sqrt{v_{t-1}} + \tau}} - \frac{1}{m} \sum_{i=1}^{m} \sum_{k=0}^{K-1} \frac{\nabla F_i(x_t)}{\sqrt{\sqrt{v_{t-1}} + \tau}} \right\|^2 \right]$$

$$\leq \frac{\eta_l K}{2} \sum_{j=1}^{d} \frac{[\nabla f(x_t)]_j^2}{\sqrt{v_{t-1,j}} + \tau} + \frac{\eta_l}{2m} \mathbb{E}_t \left[\sum_{i=1}^{m} \sum_{k=0}^{K-1} \left\| \frac{\nabla F_i(x_{i,k}^t) - \nabla F_i(x_t)}{\sqrt{\sqrt{v_{t-1}} + \tau}} \right\|^2 \right]$$

$$\leq \frac{\eta_l K}{2} \sum_{j=1}^{d} \frac{[\nabla f(x_t)]_j^2}{\sqrt{v_{t-1,j}} + \tau} + \frac{\eta_l L^2}{2m\tau} \mathbb{E}_t \left[\sum_{i=1}^{m} \sum_{k=0}^{K-1} \| x_{i,k}^t - x_t \|^2 \right] \qquad \text{using Assumption 1 and } v_{t-1} \geq 0. \qquad (6)$$

The second inequality follows from Lemma 6. The last inequality follows from L-Lipschitz nature of the gradient (Assumption 1). We now prove a lemma that bounds the "drift" of the $x_{i,k}^t$ from x_t:

Lemma 3. *For any step-size satisfying $\eta_l \leq \frac{1}{8LK}$, we can bound the drift for any $k \in \{0, \cdots, K-1\}$ as*

$$\frac{1}{m} \sum_{i=1}^{m} \mathbb{E} \| x_{i,k}^t - x_t \|^2 \leq 5K\eta_l^2 \mathbb{E} \sum_{j=1}^{d} (\sigma_{l,j}^2 + 2K\sigma_{g,j}^2) + 10K^2\eta_l^2 \mathbb{E}[\|\nabla f(x_t)))\|^2]. \qquad (7)$$

Proof. The result trivially holds for $k = 1$ since $x_{i,0}^t = x_t$ for all $i \in [m]$. We now turn our attention to the case where $k \geq 1$. To prove the above result, we observe that for any client $i \in [m]$ and $k \in [K]$,

$$
\mathbb{E}\|x_{i,k}^t - x_t\|^2 = \mathbb{E}\big\|x_{i,k-1}^t - x_t - \eta_l g_{i,k-1}^t\big\|^2
$$

$$
\leq \mathbb{E}\big\|x_{i,k-1}^t - x_t - \eta_l(g_{i,k-1}^t - \nabla F_i(x_{i,k-1}^t) + \nabla F_i(x_{i,k-1}^t) - \nabla F_i(x_t) + \nabla F_i(x_t) - \nabla f(x_t) + \nabla f(x_t))\big\|^2
$$

$$
\leq \left(1 + \frac{1}{2K-1}\right)\mathbb{E}\big\|x_{i,k-1}^t - x_t\big\|^2 + \mathbb{E}\big\|\eta_l(g_{i,k-1}^t - \nabla F_i(x_{i,k-1}^t))\big\|^2
$$

$$
+ 6K\mathbb{E}[\|\eta_l(\nabla F_i(x_{i,k-1}^t) - \nabla F_i(x_t))\|^2] + 6K\mathbb{E}[\|\eta_l(\nabla F_i(x_t) - \nabla f(x_t))\|^2] + 6K\mathbb{E}[\|\eta_l \nabla f(x_t))\|^2]
$$

The first inequality uses the fact that $g_{k-1,i}^t$ is an unbiased estimator of $\nabla F_i(x_{i,k-1}^t)$ and Lemma 7. The above quantity can be further bounded by the following:

$$
\mathbb{E}\|x_{i,k}^t - x_t\|^2 \leq \left(1 + \frac{1}{2K-1}\right)\mathbb{E}\|x_{i,k-1}^t - x_t\|^2 + \eta_l^2\mathbb{E}\sum_{j=1}^d \sigma_{l,j}^2 + 6K\eta_l^2\mathbb{E}\|L(x_{i,k-1}^t - x_t)\|^2
$$

$$
+ 6K\mathbb{E}[\|\eta_l(\nabla F_i(x_t) - \nabla f(x_t))\|^2] + 6K\mathbb{E}[\|\eta_l \nabla f(x_t))\|^2]
$$

$$
= \left(1 + \frac{1}{2K-1} + 6K\eta_l^2 L^2\right)\mathbb{E}\|(x_{i,k-1}^t - x_t)\|^2 + \eta_l^2\mathbb{E}\sum_{j=1}^d \sigma_{l,j}^2
$$

$$
+ 6K\mathbb{E}[\|\eta_l(\nabla F_i(x_t) - \nabla f(x_t))\|^2] + 6K\eta_l^2\mathbb{E}[\|\nabla f(x_t))\|^2]
$$

Here, the first inequality follows from Assumption 1 and 2. Averaging over the clients i, we obtain the following:

$$
\frac{1}{m}\sum_{i=1}^m \mathbb{E}\|x_{i,k}^t - x_t\|^2 \leq \left(1 + \frac{1}{2K-1} + 6K\eta_l^2 L^2\right)\frac{1}{m}\sum_{i=1}^m \mathbb{E}\|x_{i,k-1}^t - x_t\|^2 + \eta_l^2\mathbb{E}\sum_{j=1}^d \sigma_{l,j}^2
$$

$$
+ \frac{6K}{m}\sum_{i=1}^m \mathbb{E}[\|\eta_l(\nabla F_i(x_t) - \nabla f(x_t))\|^2] + 6K\eta_l^2\mathbb{E}[\|\nabla f(x_t))\|^2]
$$

$$
\leq \left(1 + \frac{1}{2K-1} + 6K\eta_l^2 L^2\right)\frac{1}{m}\sum_{i=1}^m \mathbb{E}\|x_{i,k-1}^t - x_t\|^2 + \eta_l^2\mathbb{E}\sum_{j=1}^d (\sigma_{l,j}^2 + 6K\sigma_{g,j}^2)
$$

$$
+ 6K\eta_l^2\mathbb{E}[\|\nabla f(x_t))\|^2]
$$

From the above, we get the following inequality:

$$
\frac{1}{m}\sum_{i=1}^m \mathbb{E}\|x_{i,k}^t - x_t\|^2 \leq \left(1 + \frac{1}{K-1}\right)\frac{1}{m}\sum_{i=1}^m \mathbb{E}\|x_{i,k-1}^t - x_t\|^2 + \eta_l^2\mathbb{E}\sum_{j=1}^d (\sigma_{l,j}^2 + 2K\sigma_{g,j}^2)
$$

$$
+ 2K\eta_l^2\mathbb{E}[\|\nabla f(x_t))\|^2]
$$

Unrolling the recursion, we obtain the following:

$$
\frac{1}{m}\sum_{i=1}^m \mathbb{E}\|x_{i,k}^t - x_t\|^2 \leq \sum_{p=0}^{k-1}\left(1 + \frac{1}{K-1}\right)^p\left[\eta_l^2\mathbb{E}\sum_{j=1}^d (\sigma_{l,j}^2 + 6K\sigma_{g,j}^2) + 6K\eta_l^2\mathbb{E}[\|\nabla f(x_t))\|^2]\right]
$$

$$
\leq (K-1) \times \left[\left(1 + \frac{1}{K-1}\right)^K - 1\right] \times \left[\eta_l^2\mathbb{E}\sum_{j=1}^d (\sigma_{l,j}^2 + 6K\sigma_{g,j}^2) + 6K\eta_l^2\mathbb{E}[\|\nabla f(x_t))\|^2]\right]
$$

$$
\leq \left[5K\eta_l^2\mathbb{E}\sum_{j=1}^d (\sigma_{l,j}^2 + 6K\sigma_{g,j}^2) + 30K^2\eta_l^2\mathbb{E}[\|\nabla f(x_t))\|^2]\right],
$$

concluding the proof of Lemma 3. The last inequality uses the fact that $(1 + \frac{1}{K-1})^K \leq 5$ for $K > 1$. $\qquad\square$

Using the above lemma in Equation 6 and the fact that $\eta_l \leq \frac{1}{8KL}$, we can bound T_3 in the following manner:

$$
\begin{aligned}
T_3 &\leq \frac{\eta_l K}{2} \sum_{j=1}^{d} \frac{[\nabla f(x_t)]_j^2}{\sqrt{v_{t-1,j}} + \tau} + \frac{\eta_l L^2}{2m\tau} \mathbb{E}_t \left[\sum_{i=1}^{m} \sum_{k=0}^{K-1} \sum_{j=1}^{d} ([x_{i,k}^t]_j - [x_t]_j)^2 \right] \\
&\leq \frac{\eta_l K}{2} \sum_{j=1}^{d} \frac{[\nabla f(x_t)]_j^2}{\sqrt{v_{t-1,j}} + \tau} + \frac{\eta_l K L^2}{2\tau} \left[5K\eta_l^2 \mathbb{E} \sum_{j=1}^{d} (\sigma_{l,j}^2 + 6K\sigma_{g,j}^2) + \frac{5}{32L^2} \mathbb{E}[\|\nabla f(x_t)))\|^2] \right] \\
&\leq \frac{3\eta_l K}{4} \sum_{j=1}^{d} \frac{[\nabla f(x_t)]_j^2}{\sqrt{v_{t-1,j}} + \tau} + \frac{5\eta_l^3 K^2 L^2}{2\tau} \mathbb{E} \sum_{j=1}^{d} (\sigma_{l,j}^2 + 6K\sigma_{g,j}^2)
\end{aligned}
$$

Using the above bound in Equation 5, we get

$$
T_1 \leq -\frac{\eta_l K}{4} \sum_{j=1}^{d} \frac{[\nabla f(x_t)]_j^2}{\sqrt{v_{t-1,j}} + \tau} + \frac{5\eta_l^3 K^2 L^2}{2\tau} \mathbb{E} \sum_{j=1}^{d} (\sigma_{l,j}^2 + 6K\sigma_{g,j}^2) \tag{8}
$$

Putting the pieces together Substituting in Equation (3), bounds T_1 in Equation (8) and bound T_2 in Equation (4), we obtain

$$
\begin{aligned}
\mathbb{E}_t[f(x_{t+1})] &\leq f(x_t) + \eta \times \left[-\frac{\eta_l K}{4} \sum_{j=1}^{d} \frac{[\nabla f(x_t)]_j^2}{\sqrt{v_{t-1,j}} + \tau} + \frac{5\eta_l^3 K^2 L^2}{2\tau} \mathbb{E} \sum_{j=1}^{d} (\sigma_{l,j}^2 + 6K\sigma_{g,j}^2) \right] \\
&\quad + \eta \times \mathbb{E} \sum_{j=1}^{d} \frac{\eta_l K G^2}{\tau} \left[\frac{\Delta_{t,j}^2}{\sum_{l=0}^{t} \Delta_{l,j}^2 + \tau^2} \right] + \frac{\eta^2}{2} \sum_{j=1}^{d} L \mathbb{E} \left[\frac{\Delta_{t,j}^2}{\sum_{l=0}^{t} \Delta_{l,j}^2 + \tau^2} \right].
\end{aligned} \tag{9}
$$

Rearranging the above inequality and summing it from $t = 0$ to $T - 1$, we get

$$
\begin{aligned}
\sum_{t=0}^{T-1} \frac{\eta_l K}{4} \sum_{j=1}^{d} \mathbb{E} \frac{[\nabla f(x_t)]_j^2}{\sqrt{v_{t-1,j}} + \tau} &\leq \frac{f(x_0) - \mathbb{E}[f(x_T)]}{\eta} + \frac{5\eta_l^3 K^2 L^2 T}{2\tau} \sum_{j=1}^{d} (\sigma_{l,j}^2 + 6K\sigma_{g,j}^2) \\
&\quad + \sum_{t=0}^{T-1} \mathbb{E} \sum_{j=1}^{d} \left(\frac{\eta_l K G^2}{\tau} + \frac{\eta L}{2} \right) \times \left[\frac{\Delta_{t,j}^2}{\sum_{l=0}^{t} \Delta_{l,j}^2 + \tau^2} \right]
\end{aligned} \tag{10}
$$

The first inequality uses simple telescoping sum. For completing the proof, we need the following result.

Lemma 4. *The following upper bound holds for Algorithm 2 (*FEDADAGRAD*):*

$$
\begin{aligned}
\mathbb{E} \sum_{t=0}^{T-1} \sum_{j=1}^{d} \frac{\Delta_{t,j}^2}{\sum_{l=0}^{t} \Delta_{l,j}^2 + \tau^2} &\leq \left[\min \left\{ d + \sum_{j=1}^{d} \log \left(1 + \frac{\eta_l^2 K^2 G^2 T}{\tau^2} \right) \right. \right. \\
&\quad \left. \left. + \frac{4\eta_l^2 KT}{m\tau^2} \sum_{j=1}^{d} \sigma_{l,j}^2 + 20\eta_l^4 K^3 L^2 T \mathbb{E} \sum_{j=1}^{d} \frac{(\sigma_{l,j}^2 + 6K\sigma_{g,j}^2)}{\tau^2} + \frac{40\eta_l^4 K^2 L^2}{\tau^2} \sum_{t=0}^{T-1} \mathbb{E} \left[\|\nabla f(x_t)\|^2 \right] \right\} \right]
\end{aligned}
$$

Proof. We bound the desired quantity in the following manner:

$$
\mathbb{E} \sum_{t=0}^{T-1} \sum_{j=1}^{d} \frac{\Delta_{t,j}^2}{\sum_{l=0}^{t} \Delta_{l,j}^2 + \tau^2} \leq d + \mathbb{E} \sum_{j=1}^{d} \log \left(1 + \frac{\sum_{l=0}^{T-1} \Delta_{l,j}^2}{\tau^2} \right) \leq d + \sum_{j=1}^{d} \log \left(1 + \frac{\eta_l^2 K^2 G^2 T}{\tau^2} \right).
$$

An alternate way of the bounding this quantity is as follows:

$$\mathbb{E}\sum_{t=0}^{T-1}\sum_{j=1}^{d}\frac{\Delta_{t,j}^2}{\sum_{l=0}^{t}\Delta_{t,j}^2+\tau^2}\leq\mathbb{E}\sum_{t=0}^{T-1}\sum_{j=1}^{d}\frac{\Delta_{t,j}^2}{\tau^2}$$

$$\leq\mathbb{E}\sum_{t=0}^{T-1}\left\|\frac{\Delta_t+\eta_l K\nabla f(x_t)-\eta_l K\nabla f(x_t)}{\tau}\right\|^2$$

$$\leq 2\mathbb{E}\sum_{t=0}^{T-1}\left[\left\|\frac{\Delta_t+\eta_l K\nabla f(x_t)}{\tau}\right\|^2+\eta_l^2 K^2\left\|\frac{\nabla f(x_t)}{\tau}\right\|^2\right]$$

The first quantity in the above bound can be further bounded as follows:

$$2\mathbb{E}\sum_{t=0}^{T-1}\left\|\frac{1}{\tau}\cdot\left(-\frac{1}{m}\sum_{i=1}^{m}\sum_{k=0}^{K-1}\eta_l g_{i,k}^t+\eta_l K\nabla f(x_t)\right)\right\|^2$$

$$=2\mathbb{E}\sum_{t=0}^{T-1}\left[\left\|\frac{1}{\tau}\cdot\left(\frac{1}{m}\sum_{i=1}^{m}\sum_{k=0}^{K-1}\left(\eta_l g_{i,k}^t-\eta_l\nabla F_i(x_{i,k}^t)+\eta_l\nabla F_i(x_{i,k}^t)-\eta_l\nabla F_i(x_t)+\eta_l\nabla F_i(x_t)\right)-\eta_l K\nabla f(x_t)\right)\right\|^2\right]$$

$$=\frac{2\eta_l^2}{m^2}\sum_{t=0}^{T-1}\mathbb{E}\left[\left\|\sum_{i=1}^{m}\sum_{k=0}^{K-1}\frac{1}{\tau}\cdot\left(g_{i,k}^t-\nabla F_i(x_{i,k}^t)+\nabla F_i(x_{i,k}^t)-\nabla F_i(x_t)\right)\right\|^2\right]$$

$$\leq\frac{4\eta_l^2}{m^2}\sum_{t=0}^{T-1}\mathbb{E}\left[\left\|\sum_{i=1}^{m}\sum_{k=0}^{K-1}\frac{1}{\tau}\cdot\left(g_{i,k}^t-\nabla F_i(x_{i,k}^t)\right)\right\|^2+\left\|\sum_{i=1}^{m}\sum_{k=0}^{K-1}\frac{1}{\tau}\cdot\left(\nabla F_i(x_{i,k}^t)-\nabla F_i(x_t)\right)\right\|^2\right]$$

$$\leq\frac{4\eta_l^2 KT}{m}\sum_{j=1}^{d}\frac{\sigma_{l,j}^2}{\tau^2}+\frac{4\eta_l^2 K}{m}\sum_{i=1}^{m}\sum_{k=0}^{K-1}\sum_{t=0}^{T-1}\left\|\frac{1}{\tau}\cdot\left(\nabla F_i(x_{i,k}^t)-\nabla F_i(x_t)\right)\right\|^2$$

$$\leq\frac{4\eta_l^2 KT}{m}\sum_{j=1}^{d}\frac{\sigma_{l,j}^2}{\tau^2}+\frac{4\eta_l^2 K}{m}\sum_{i=1}^{m}\sum_{k=0}^{K-1}\sum_{t=0}^{T-1}\left\|\frac{L}{\tau}\cdot\left(x_{i,k}^t-x_t\right)\right\|^2 \qquad\text{using Assumption 1 and Assumption 2}$$

$$\leq\frac{4\eta_l^2 KT}{m\tau^2}\sum_{j=1}^{d}\sigma_{l,j}^2+20\eta_l^4 K^3 L^2 T\mathbb{E}\sum_{j=1}^{d}\frac{(\sigma_{l,j}^2+6K\sigma_{g,j}^2)}{\tau^2}+\frac{40\eta_l^4 K^4 L^2}{\tau^2}\sum_{t=0}^{T-1}\mathbb{E}\left[\|\nabla f(x_t)\|^2\right] \qquad\text{using Lemma 3.}$$

Here, the first inequality follows from simple application of the fact that $ab\leq(a^2+b^2)/2$. The result follows. $\qquad\square$

Substituting the above bound in Equation (10), we obtain:

$$\frac{\eta_l K}{4}\sum_{t=0}^{T-1}\sum_{j=1}^{d}\mathbb{E}\frac{[\nabla f(x_t)]_j^2}{\sqrt{v_{t-1,j}}+\tau}$$

$$\leq\frac{f(x_0)-\mathbb{E}[f(x_T)]}{\eta}+\frac{5\eta_l^3 K^2 L^2}{2\tau}\mathbb{E}\sum_{t=0}^{T-1}\sum_{j=1}^{d}(\sigma_{l,j}^2+6K\sigma_{g,j}^2)$$

$$+\sum_{j=1}^{d}\left(\frac{\eta_l KG^2}{\tau}+\frac{\eta L}{2}\right)\times\left[\min\left\{d+d\log\left(1+\frac{\eta_l^2 K^2 G^2 T}{\tau^2}\right)+\right.\right.$$

$$\left.\left.\frac{4\eta_l^2 KT}{m\tau^2}\sum_{j=1}^{d}\sigma_{l,j}^2+20\eta_l^4 K^3 L^2 T\mathbb{E}\sum_{j=1}^{d}\frac{(\sigma_{l,j}^2+6K\sigma_{g,j}^2)}{\tau^2}+\frac{40\eta_l^4 K^4 L^2}{\tau^2}\sum_{t=0}^{T-1}\mathbb{E}\left[\|\nabla f(x_t)\|^2\right]\right\}\right] \qquad(11)$$

We observe the following:

$$\sum_{t=0}^{T-1}\sum_{j=1}^{d}\frac{[\nabla\mathbb{E}f(x_t)]_j^2}{\sqrt{v_{t-1,j}}+\tau}\geq\sum_{t=0}^{T-1}\sum_{j=1}^{d}\mathbb{E}\frac{[\nabla f(x_t)]_j^2}{\eta_l KG\sqrt{T}+\tau}\geq\frac{T}{\eta_l KG\sqrt{T}+\tau}\min_{0\leq t\leq T}\mathbb{E}\|\nabla f(x_t)\|^2.$$

The second part of Theorem 1 follows from using the above inequality in Equation (11). Note that the first part of Theorem 1 is obtain from the part of Lemma 4. □

A.2 Proof of Theorem 2

Proof of Theorem 2. The proof strategy is similar to that of FEDADAGRAD except that we need to handle the exponential moving average in FEDADAM. We note that the update of FEDADAM is the following

$$x_{t+1}=x_t+\eta\frac{\Delta_t}{\sqrt{v_t}+\tau},$$

for all $i\in[d]$. Using the L-smooth nature of function f and the above update rule, we have the following:

$$f(x_{t+1})\leq f(x_t)+\eta\left\langle\nabla f(x_t),\frac{\Delta_t}{\sqrt{v_t}+\tau}\right\rangle+\frac{\eta^2 L}{2}\sum_{i=1}^{d}\frac{\Delta_{t,i}^2}{(\sqrt{v_{t,i}}+\tau)^2}\tag{12}$$

The second step follows simply from FEDADAM's update. We take the expectation of $f(x_{t+1})$ (over randomness at time step t) and rewrite the above inequality as:

$$\mathbb{E}_t[f(x_{t+1})]\leq f(x_t)+\eta\left\langle\nabla f(x_t),\mathbb{E}_t\left[\frac{\Delta_t}{\sqrt{v_t}+\tau}-\frac{\Delta_t}{\sqrt{\beta_2 v_{t-1}}+\tau}+\frac{\Delta_t}{\sqrt{\beta_2 v_{t-1}}+\tau}\right]\right\rangle+\frac{\eta^2 L}{2}\sum_{j=1}^{d}\mathbb{E}_t\left[\frac{\Delta_{t,j}^2}{(\sqrt{v_{t,j}}+\tau)^2}\right]$$

$$=f(x_t)+\eta\underbrace{\left\langle\nabla f(x_t),\mathbb{E}_t\left[\frac{\Delta_t}{\sqrt{\beta_2 v_{t-1}}+\tau}\right]\right\rangle}_{R_1}+\eta\underbrace{\left\langle\nabla f(x_t),\mathbb{E}_t\left[\frac{\Delta_t}{\sqrt{v_t}+\tau}-\frac{\Delta_t}{\sqrt{\beta_2 v_{t-1}}+\tau}\right]\right\rangle}_{R_2}$$

$$+\frac{\eta^2 L}{2}\sum_{j=1}^{d}\mathbb{E}_t\left[\frac{\Delta_{t,j}^2}{(\sqrt{v_{t,j}}+\tau)^2}\right]\tag{13}$$

Bounding R_2. We observe the following about R_2:

$$R_2=\mathbb{E}_t\sum_{j=1}^{d}[\nabla f(x_t)]_j\times\left[\frac{\Delta_{t,j}}{\sqrt{v_{t,j}}+\tau}-\frac{\Delta_{t,j}}{\sqrt{\beta_2 v_{t-1,j}}+\tau}\right]$$

$$=\mathbb{E}_t\sum_{j=1}^{d}[\nabla f(x_t)]_j\times\Delta_{t,j}\times\left[\frac{\sqrt{\beta_2 v_{t-1,j}}-\sqrt{v_{t,j}}}{(\sqrt{v_{t,j}}+\tau)(\sqrt{\beta_2 v_{t-1,j}}+\tau)}\right]$$

$$=\mathbb{E}_t\sum_{j=1}^{d}[\nabla f(x_t)]_j\times\Delta_{t,j}\times\left[\frac{-(1-\beta_2)\Delta_{t,j}^2}{(\sqrt{v_{t,j}}+\tau)(\sqrt{\beta_2 v_{t-1,j}}+\tau)(\sqrt{\beta_2 v_{t-1,j}}+\sqrt{v_{t,j}})}\right]$$

$$\leq(1-\beta_2)\mathbb{E}_t\sum_{j=1}^{d}|\nabla f(x_t)]_j|\times|\Delta_{t,j}|\times\left[\frac{\Delta_{t,j}^2}{(\sqrt{v_{t,j}}+\tau)(\sqrt{\beta_2 v_{t-1,j}}+\tau)(\sqrt{\beta_2 v_{t-1,j}}+\sqrt{v_{t,j}})}\right]$$

$$\leq\sqrt{1-\beta_2}\mathbb{E}_t\sum_{j=1}^{d}|\nabla f(x_t)]_j|\times\left[\frac{\Delta_{t,j}^2}{\sqrt{v_{t,j}}+\tau)(\sqrt{\beta_2 v_{t-1,j}}+\tau)}\right]$$

$$\leq\sqrt{1-\beta_2}\mathbb{E}_t\sum_{j=1}^{d}\frac{G}{\tau}\times\left[\frac{\Delta_{t,j}^2}{\sqrt{v_{t,j}}+\tau}\right].$$

Bounding R_1. The term R_1 can be bounded as follows:

$$
\begin{aligned}
R_1 &= \left\langle \nabla f(x_t), \mathbb{E}_t \left[\frac{\Delta_t}{\sqrt{\beta_2 v_{t-1}} + \tau} \right] \right\rangle \\
&= \left\langle \frac{\nabla f(x_t)}{\sqrt{\beta_2 v_{t-1}} + \tau}, \mathbb{E}_t \left[\Delta_t - \eta_l K \nabla f(x_t) + \eta_l K \nabla f(x_t) \right] \right\rangle \\
&= -\eta_l K \sum_{j=1}^{d} \frac{[\nabla f(x_t)]_j^2}{\sqrt{\beta_2 v_{t-1,j}} + \tau} + \underbrace{\left\langle \frac{\nabla f(x_t)}{\sqrt{\beta_2 v_{t-1}} + \tau}, \mathbb{E}_t \left[\Delta_t + \eta_l K \nabla f(x_t) \right] \right\rangle}_{R_3}.
\end{aligned}
\tag{14}
$$

Bounding R_3. The term R_3 can be bounded in exactly the same way as term T_3 in proof of Theorem 1:

$$
R_3 \leq \frac{\eta_l K}{2} \sum_{j=1}^{d} \frac{[\nabla f(x_t)]_j^2}{\sqrt{\beta_2 v_{t-1,j}} + \tau} + \frac{\eta_l L^2}{2m\tau} \mathbb{E}_t \left[\sum_{i=1}^{m} \sum_{k=0}^{K-1} \| x_{i,k}^t - x_t \|^2 \right]
$$

Substituting the above inequality in Equation (14), we get

$$
R_1 \leq -\frac{\eta_l K}{2} \sum_{j=1}^{d} \frac{[\nabla f(x_t)]_j^2}{\sqrt{\beta_2 v_{t-1,j}} + \tau} + \frac{\eta_l L^2}{2m\tau} \mathbb{E}_t \left[\sum_{i=1}^{m} \sum_{k=0}^{K-1} \| x_{i,k}^t - x_t \|^2 \right]
$$

Using Lemma 3, we obtain the following bound on R_1:

$$
R_1 \leq -\frac{\eta_l K}{4} \sum_{j=1}^{d} \frac{[\nabla f(x_t)]_j^2}{\sqrt{\beta_2 v_{t-1,j}} + \tau} + \frac{5\eta_l^3 K^2 L^2}{2\tau} \mathbb{E}_t \sum_{j=1}^{d} (\sigma_{l,j}^2 + 6K\sigma_{g,j}^2)
\tag{15}
$$

Putting pieces together. Substituting bounds R_1 and R_2 in Equation (13), we have

$$
\begin{aligned}
\mathbb{E}_t[f(x_{t+1})] \leq f(x_t) &- \frac{\eta \eta_l K}{4} \sum_{j=1}^{d} \frac{[\nabla f(x_t)]_j^2}{\sqrt{\beta_2 v_{t-1,j}} + \tau} + \frac{5\eta \eta_l^3 K^2 L^2}{2\tau} \mathbb{E} \sum_{j=1}^{d} (\sigma_{l,j}^2 + 6K\sigma_{g,j}^2) \\
&+ \left(\frac{\eta \sqrt{1-\beta_2} G}{\tau} \right) \sum_{j=1}^{d} \mathbb{E}_t \left[\frac{\Delta_{t,j}^2}{\sqrt{v_{t,j}} + \tau)} \right] + \left(\frac{\eta^2 L}{2} \right) \sum_{j=1}^{d} \mathbb{E}_t \left[\frac{\Delta_{t,j}^2}{v_{t,j} + \tau^2)} \right]
\end{aligned}
$$

Summing over $t = 0$ to $T - 1$ and using telescoping sum, we have

$$
\begin{aligned}
\mathbb{E}[f(x_T)] \leq f(x_0) &- \frac{\eta \eta_l K}{4} \sum_{t=0}^{T-1} \sum_{j=1}^{d} \mathbb{E} \frac{[\nabla f(x_t)]_j^2}{\sqrt{\beta_2 v_{t-1,j}} + \tau} + \frac{5\eta \eta_l^3 K^2 L^2 T}{2\tau} \mathbb{E} \sum_{j=1}^{d} (\sigma_{l,j}^2 + 6K\sigma_{g,j}^2) \\
&\left(\frac{\eta \sqrt{1-\beta_2} G}{\tau} \right) \sum_{t=0}^{T-1} \sum_{j=1}^{d} \mathbb{E} \left[\frac{\Delta_{t,j}^2}{\sqrt{v_{t,j}} + \tau)} \right] + \left(\frac{\eta^2 L}{2} \right) \sum_{t=0}^{T-1} \sum_{j=1}^{d} \mathbb{E} \left[\frac{\Delta_{t,j}^2}{v_{t,j} + \tau^2)} \right]
\end{aligned}
\tag{16}
$$

To bound this term further, we need the following result.

Lemma 5. *The following upper bound holds for Algorithm 2 (*FEDYOGI*):*

$$
\sum_{t=0}^{T-1} \sum_{j=1}^{d} \mathbb{E} \left[\frac{\Delta_{t,j}^2}{(v_{t,j} + \tau^2)} \right] \leq \frac{4\eta_l^2 KT}{m\tau^2} \sum_{j=1}^{d} \sigma_{l,j}^2 + \frac{20\eta_l^4 K^3 L^2 T}{\tau^2} \mathbb{E} \sum_{j=1}^{d} (\sigma_{l,j}^2 + 6K\sigma_{g,j}^2) + \frac{40\eta_l^4 K^4 L^2}{\tau^2} \sum_{t=0}^{T-1} \mathbb{E} \left[\| \nabla f(x_t) \|^2 \right]
$$

Proof.

$$\mathbb{E} \sum_{t=0}^{T-1} \sum_{j=1}^{d} \frac{\Delta_{t,j}^2}{(1-\beta_2) \sum_{l=0}^{t} \beta_2^{t-l} \Delta_{t,j}^2 + \tau^2} \leq \mathbb{E} \sum_{t=0}^{T-1} \sum_{j=1}^{d} \frac{\Delta_{t,j}^2}{\tau^2}$$

The rest of the proof follows along the lines of proof of Lemma 4. Using the same argument, we get

$$\sum_{j=1}^{d} \mathbb{E}\left[\frac{\Delta_{t,j}^2}{(v_{t,j}+\tau^2)}\right] \leq \frac{4\eta_l^2 KT}{m\tau^2} \sum_{j=1}^{d} \sigma_{l,j}^2 + \frac{20\eta_l^4 K^3 L^2 T}{\tau^2} \mathbb{E} \sum_{j=1}^{d} (\sigma_{l,j}^2 + 6K\sigma_{g,j}^2)$$
$$+ \frac{40\eta_l^4 K^4 L^2}{\tau^2} \sum_{t=0}^{T-1} \mathbb{E}\left[\|\nabla f(x_t)\|^2\right],$$

which is the desired result. □

Substituting the bound obtained from above lemma in Equation (16) and using a similar argument for bounding

$$\left(\frac{\eta\sqrt{1-\beta_2}G}{\tau}\right) \sum_{t=0}^{T-1} \sum_{j=1}^{d} \mathbb{E}\left[\frac{\Delta_{t,j}^2}{\sqrt{v_{t,j}}+\tau)}\right],$$

we obtain

$$\mathbb{E}_t[f(x_T)] \leq f(x_0) - \frac{\eta\eta_l K}{8} \sum_{t=0}^{T-1} \sum_{j=1}^{d} \frac{[\nabla f(x_t)]_j^2}{\sqrt{\beta_2 v_{t-1,j}}+\tau} + \frac{5\eta\eta_l^3 K^2 L^2 T}{2\tau} \mathbb{E} \sum_{j=1}^{d} (\sigma_{l,j}^2 + 6K\sigma_{g,j}^2)$$
$$+ \left(\eta\sqrt{1-\beta_2}G + \frac{\eta^2 L}{2}\right) \times \left[\frac{4\eta_l^2 KT}{m\tau^2} \sum_{j=1}^{d} \sigma_{l,j}^2 + \frac{20\eta_l^4 K^4 L^2 T}{\tau^2} \mathbb{E} \sum_{j=1}^{d} (\sigma_{l,j}^2 + 6K\sigma_{g,j}^2)\right]$$

The above inequality is obtained due to the fact that:

$$\left(\sqrt{1-\beta_2}G + \frac{\eta L}{2}\right) \frac{40\eta_l^4 K^4 L^2}{\tau^2} \leq \frac{\eta_l K}{16} \left(\frac{1}{\sqrt{\beta_2}\eta_l KG} + \frac{1}{\tau}\right).$$

The above condition follows from the condition on η_l in Theorem 2. We also observe the following:

$$\sum_{t=0}^{T-1} \sum_{j=1}^{d} \frac{[\nabla f(x_t)]_j^2}{\sqrt{\beta_2 v_{t-1,j}}+\tau} \geq \sum_{t=0}^{T-1} \sum_{j=1}^{d} \frac{[\nabla f(x_t)]_j^2}{\sqrt{\beta_2}\eta_l KG+\tau} \geq \frac{T}{\sqrt{\beta_2}\eta_l KG+\tau} \min_{0 \leq t \leq T} \|\nabla f(x_t)\|^2.$$

Substituting this bound in the above equation yields the desired result. □

A.3 Auxiliary Lemmatta

Lemma 6. *For random variables $z_1, \ldots, z_r$, we have*

$$\mathbb{E}\left[\|z_1 + \ldots + z_r\|^2\right] \leq r\mathbb{E}\left[\|z_1\|^2 + \ldots + \|z_r\|^2\right].$$

Lemma 7. *For independent, mean 0 random variables $z_1, \ldots, z_r$, we have*

$$\mathbb{E}\left[\|z_1 + \ldots + z_r\|^2\right] = \mathbb{E}\left[\|z_1\|^2 + \ldots + \|z_r\|^2\right].$$

B Algorithms

In Algorithm 3, we give a simplified version of the FEDAVG algorithm by McMahan et al. (2017), that applies to the setup given in Section 2. We write $\text{SGD}_K(x_t, \eta_l, F_i)$ to denote K steps of SGD on gradients $\nabla f_i(x, z)$ for $z \sim \mathcal{D}_i$ with (local) learning rate η_l, starting from x_t. As noted in Section 2, Algorithm 3 is the special case of Algorithm 1 where CLIENTOPT is SGD, and SERVEROPT is SGD with learning rate 1.

Algorithm 3 Simplified FEDAVG

Input: x_0
for $t = 0, \cdots, T - 1$ **do**
    Sample a subset $\mathcal{S}$ of clients
    $x_i^t = x_t$
    for each client $i \in \mathcal{S}$ **in parallel do**
        $x_i^t = \text{SGD}_K(x_t, \eta_l, F_i)$ for $i \in \mathcal{S}$ (in parallel)
    $x_{t+1} = \frac{1}{|\mathcal{S}|} \sum_{i \in \mathcal{S}} x_i^t$

While Algorithms 1, 2, and 3 are useful for understanding relations between these optimizers, we are also interested in practical versions of these algorithms. In particular, these algorithms are stated in terms of a kind of 'gradient oracle', where we compute unbiased estimates of the client's gradient. In practical scenarios, we often only have access to finite data samples, the number of which may vary between clients.

Instead, we assume that in (1), each client distribution $\mathcal{D}_i$ is the uniform distribution over some finite set D_i of size n_i. The n_i may vary significantly between clients, requiring extra care when implementing federated optimization methods. We assume the set D_i is partitioned into a collection of batches $\mathcal{B}_i$, each of size B. For $b \in \mathcal{B}_i$, we let $f_i(x; b)$ denote the average loss on this batch at x with corresponding gradient $\nabla f_i(x; b)$. Thus, $\nabla f_i(x; b)$ is an unbiased estimate of $\nabla F_i(x)$.

When training, instead of uniformly using K gradient steps, as in Algorithm 1, we will instead perform E epochs of training over each client's dataset. Additionally, we will take a weighted average of the client updates, where we weight according to the number of examples n_i in each client's dataset. This leads to a batched data version of FEDOPT in Algorithm 4, and a batched data version of FEDADAGRAD, FEDADAM, and FEDYOGI given in Algorithm 5. In the latter, we also give the full version of the algorithms that includes the use of momentum, governed by a parameter β_1.

Algorithm 4 FEDOPT - Batched data

Input: x_0, CLIENTOPT, SERVEROPT
for $t = 0, \cdots, T - 1$ **do**
    Sample a subset $\mathcal{S}$ of clients
    $x_i^t = x_t$
    for each client $i \in \mathcal{S}$ **in parallel do**
        for $e = 1, \ldots, E$ **do**
            for $b \in \mathcal{B}_i$ **do**
                $g_i^t = \nabla f_i(x_i^t; b)$
                $x_i^t = \text{CLIENTOPT}(x_i^t, g_i^t, \eta_l, t)$
        $\Delta_i^t = x_i^t - x_t$
    $n = \sum_{i \in \mathcal{S}} n_i, \ \Delta_t = \sum_{i \in \mathcal{S}} \frac{n_i}{n} \Delta_i^t$
    $x_{t+1} = \text{SERVEROPT}(x_t, -\Delta_t, \eta, t)$

In Section 5, we use Algorithm 4 when implementing FEDAVG and FEDAVGM. In particular, FEDAVG and FEDAVGM correspond to Algorithm 4 where CLIENTOPT and SERVEROPT are SGD. FEDAVG uses vanilla SGD on the server, while FEDAVGM uses SGD with a momentum parameter of 0.9. In both methods, we tune both client learning rate η_l and server learning rate η. This means that the version of FEDAVG used in all experiments is strictly more general than that in (McMahan et al., 2017), which corresponds to FEDOPT where CLIENTOPT and SERVEROPT are SGD, and SERVEROPT has a learning rate of 1.

Algorithm 5 **FEDADAGRAD** , **FEDYOGI** , and **FEDADAM** - Batched data

---

Input: $x_0, v_{-1} \geq \tau^2$, optional $\beta_1, \beta_2 \in [0, 1)$ for FEDYOGI and FEDADAM

for $t = 0, \cdots, T - 1$ **do**

    Sample a subset $\mathcal{S}$ of clients

    $x_i^t = x_t$

    for each client $i \in \mathcal{S}$ **in parallel do**

        for $e = 1, \ldots, E$ **do**

            for $b \in \mathcal{B}_i$ **do**

                $x_i^t = x_i^t - \eta_l \nabla f_i(x_i^t; b)$

        $\Delta_i^t = x_i^t - x_t$

    $n = \sum_{i \in \mathcal{S}} n_i, \ \Delta_t = \sum_{i \in \mathcal{S}} \frac{n_i}{n} \Delta_i^t$

    $\Delta_t = \beta_1 \Delta_{t-1} + (1 - \beta_1) \Delta_t$

    $v_t = v_{t-1} + \Delta_t^2$ **(FEDADAGRAD)**

    $v_t = v_{t-1} - (1 - \beta_2) \Delta_t^2 \, \mathrm{sign}(v_{t-1} - \Delta_t^2)$ **(FEDYOGI)**

    $v_t = \beta_2 v_{t-1} + (1 - \beta_2) \Delta_t^2$ **(FEDADAM)**

    $x_{t+1} = x_t + \eta \frac{\Delta_t}{\sqrt{v_t} + \tau}$

We use Algorithm 5 for all implementations FEDADAGRAD, FEDADAM, and FEDYOGI in Section 5. For FEDADA-GRAD, we set $\beta_1 = \beta_2 = 0$ (as typical versions of ADAGRAD do not use momentum), while for FEDADAM and FEDYOGI we set $\beta_1 = 0.9, \beta_2 = 0.99$. While these parameters are generally good choices (Zaheer et al., 2018), we emphasize that better results may be obtainable by tuning these parameters.

C Dataset & Models

Here we provide detailed description of the datasets and models used in the paper. We use federated versions of vision datasets EMNIST (Cohen et al., 2017) and CIFAR-100 (Krizhevsky and Hinton, 2009), and language modeling datasets Shakespeare (McMahan et al., 2017) and StackOverflow (Authors, 2019). Statistics for the training datasets can be found in Table 1. We give descriptions of the datasets, models, and tasks below.

C.1 CIFAR-100

We introduce a federated version of CIFAR-100 by randomly partitioning the training data among 500 clients, with each client receiving 100 examples. While Hsu et al. (2019) used latent Dirichlet allocation (LDA) over the fine labels of CIFAR-100 to create a federated dataset, we use a two step LDA process over the coarse and fine labels. We randomly partition the data to reflect the "coarse" and "fine" label structure of CIFAR-100 by using the Pachinko Allocation Method (PAM) (Li and McCallum, 2006). This creates more realistic client datasets, whose label distributions better resemble practical heterogeneous client datasets. We have made publicly available the specific federated version of CIFAR-100 we used for all experiments.[3] For complete details on how the dataset was created, see Appendix F.

We train a modified ResNet-18 on this dataset, where the batch normalization layers are replaced by group normalization layers (Wu and He, 2018), with two groups. As shown by Hsieh et al. (2019), group normalization can lead to significant gains in accuracy over batch normalization in federated settings.

Preprocessing CIFAR-100 consists of images with 3 channels of 32×32 pixels each. Each pixel is represented by an unsigned int8. As is standard with CIFAR-100, we perform preprocessing on both training and test images. For training images, we perform a random crop to shape $(24, 24, 3)$, followed by a random horizontal flip. For testing

---

[3]https://www.tensorflow.org/federated/api_docs/python/tff/simulation/datasets/cifar100

images, we centrally crop the image to $(24, 24, 3)$. For both training and testing images, we then normalize the pixel values according to their mean and standard deviation. Namely, given an image x, we compute $(x - \mu)/\sigma$ where μ is the average of the pixel values in x, and σ is the standard deviation.

C.2 EMNIST

EMNIST consists of images of digits and upper and lower case English characters, with 62 total classes. The federated version of EMNIST (Caldas et al., 2018) partitions the digits by their author. The dataset has natural heterogeneity stemming from the writing style of each person. We perform two distinct tasks on EMNIST, autoencoder training (EMNIST AE) and character recognition (EMNIST CR). For EMNIST AE, we train the "MNIST" autoencoder (Zaheer et al., 2018). This is a densely connected autoencoder with layers of size $(28 \times 28) - 1000 - 500 - 250 - 30$ and a symmetric decoder. A full description of the model is in Table 6. For EMNIST CR, we use a convolutional network. The network has two convolutional layers (with 3×3 kernels), max pooling, and dropout, followed by a 128 unit dense layer. A full description of the model is in Table 7.

Table 6: EMNIST autoencoder model architecture. We use a sigmoid activation at all dense layers.

Layer	Output Shape	# of Trainable Parameters
Input	784	0
Dense	1000	785000
Dense	500	500500
Dense	250	125250
Dense	30	7530
Dense	250	7750
Dense	500	125500
Dense	1000	501000
Dense	784	784784

Table 7: EMNIST character recognition model architecture.

Layer	Output Shape	# of Trainable Parameters	Activation	Hyperparameters
Input	$(28, 28, 1)$	0		
Conv2d	$(26, 26, 32)$	320		kernel size = 3; strides=$(1, 1)$
Conv2d	$(24, 24, 64)$	18496	ReLU	kernel size = 3; strides=$(1, 1)$
MaxPool2d	$(12, 12, 64)$	0		pool size= $(2, 2)$
Dropout	$(12, 12, 64)$	0		$p = 0.25$
Flatten	9216	0		
Dense	128	1179776		
Dropout	128	0		$p = 0.5$
Dense	62	7998	softmax	

C.3 Shakespeare

Shakespeare is a language modeling dataset built from the collective works of William Shakespeare. In this dataset, each client corresponds to a speaking role with at least two lines. The dataset consists of 715 clients. Each client's lines are partitioned into training and test sets. Here, the task is to do next character prediction. We use an RNN that

first takes a series of characters as input and embeds each of them into a learned 8-dimensional space. The embedded characters are then passed through 2 LSTM layers, each with 256 nodes, followed by a densely connected softmax output layer. We split the lines of each speaking role into into sequences of 80 characters, padding if necessary. We use a vocabulary size of 90; 86 for the characters contained in the Shakespeare dataset, and 4 extra characters for padding, out-of-vocabulary, beginning of line and end of line tokens. We train our model to take a sequence of 80 characters, and predict a sequence of 80 characters formed by shifting the input sequence by one (so that its last character is the new character we are actually trying to predict). Therefore, our output dimension is 80×90. A full description of the model is in Table 8.

Table 8: Shakespeare model architecture.

Layer	Output Shape	# of Trainable Parameters
Input	80	0
Embedding	$(80, 8)$	720
LSTM	$(80, 256)$	271360
LSTM	$(80, 256)$	525312
Dense	$(80, 90)$	23130

C.4 Stack Overflow

Stack Overflow is a language modeling dataset consisting of question and answers from the question and answer site, Stack Overflow. The questions and answers also have associated metadata, including tags. The dataset contains 342,477 unique users which we use as clients. We perform two tasks on this dataset: tag prediction via logistic regression (Stack Overflow LR, SO LR for short), and next-word prediction (Stack Overflow NWP, SO NWP for short). For both tasks, we restrict to the 10,000 most frequently used words. For Stack Overflow LR, we restrict to the 500 most frequent tags and adopt a one-versus-rest classification strategy, where each question/answer is represented as a bag-of-words vector (normalized to have sum 1).

For Stack Overflow NWP, we restrict each client to the first 128 sentences in their dataset. We also perform padding and truncation to ensure that sentences have 20 words. We then represent the sentence as a sequence of indices corresponding to the 10,000 frequently used words, as well as indices representing padding, out-of-vocabulary words, beginning of sentence, and end of sentence. We perform next-word-prediction on these sequences using an RNN that embeds each word in a sentence into a learned 96-dimensional space. It then feeds the embedded words into a single LSTM layer of hidden dimension 670, followed by a densely connected softmax output layer. A full description of the model is in Table 9. The metric used in the main body is the top-1 accuracy over the proper 10,000-word vocabulary; that is, it does not include padding, out-of-vocab, or beginning or end of sentence tokens.

Table 9: Stack Overflow next word prediction model architecture.

Layer	Output Shape	# of Trainable Parameters
Input	20	0
Embedding	$(20, 96)$	960384
LSTM	$(20, 670)$	2055560
Dense	$(20, 96)$	64416
Dense	$(20, 10004)$	970388

D   Experiment Hyperparameters

D.1   Hyperparameter tuning

Throughout our experiments, we compare the performance of different instantiations of Algorithm 1 that use different server optimizers. We use SGD, SGD with momentum (denoted SGDM), ADAGRAD, ADAM, and YOGI. For the client optimizer, we use mini-batch SGD throughout. For all tasks, we tune the client learning rate η_l and server learning rate η by using a large grid search. Full descriptions of the per-task server and client learning rate grids are given in Appendix D.2.

We use the version of FEDADAGRAD, FEDADAM, and FEDYOGI in Algorithm 5. We let $\beta_1 = 0$ for FEDADAGRAD, and we let $\beta_1 = 0.9, \beta_2 = 0.99$ for FEDADAM, and FEDYOGI. For FEDAVG and FEDAVGM, we use Algorithm 4, where CLIENTOPT, SERVEROPT are SGD. For FEDAVGM, the server SGD optimizer uses a momentum parameter of 0.9. For FEDADAGRAD, FEDADAM, and FEDYOGI, we tune the parameter τ in Algorithm 5. For all tasks, we tune τ over the grid:

$$\tau \in \{10^{-7}, 10^{-6}, \ldots, 10^{-1}\}.$$

D.2   Client and server learning rate grids

Below, we give the client learning rate (η_l in Algorithm 1) and server learning rate (η in Algorithm 1) grids used for each task. These grids were chosen based on an initial evaluation over the grids

$$\eta_l \in \{10^{-3}, 10^{-2.5}, 10^{-2}, \ldots, 10^{0.5}\}$$
$$\eta \in \{10^{-1.5}, 10^{-1}, 10^{-0.5}, \ldots, 10^1\}$$

These grids were then refined for Stack Overflow and EMNIST AE in an attempt to ensure that the best client/server learning rate combinations for each optimizer was contained in the interior of the learning rate grids. We found that EMNIST AE required a finer grid, while Stack Overflow LR required searching over much larger learning rates. The final grids were as follows:

CIFAR-100:
$$\eta_l \in \{10^{-3}, 10^{-2.5}, 10^{-2}, \ldots, 10^{0.5}\}$$
$$\eta \in \{10^{-1.5}, 10^{-1}, 10^{-0.5}, \ldots, 10^1\}$$

EMNIST AE:
$$\eta_1 \in \{0.01, 0.05, 0.1, 0.5, 1, 5, 10\}$$
$$\eta \in \{10^{-3}, 10^{-2}, 10^{-1}, 1, 10\}$$

EMNIST CR:
$$\eta_l \in \{10^{-3}, 10^{-2.5}, 10^{-2}, \ldots, 10^{0.5}\}$$
$$\eta \in \{10^{-1.5}, 10^{-1}, 10^{-0.5}, \ldots, 10^1\}$$

Shakespeare:
$$\eta_l \in \{10^{-3}, 10^{-2.5}, 10^{-2}, \ldots, 10^{0.5}\}$$
$$\eta \in \{10^{-1.5}, 10^{-1}, 10^{-0.5}, \ldots, 10^1\}$$

StackOverflow LR:
$$\eta_l \in \{10^{-1.5}, 10^{-2.5}, 10^{-2}, \ldots, 10^2\}$$
$$\eta \in \{10^{-1.5}, 10^{-1}, 10^{-0.5}, \ldots, 10^{1.5}\}$$

StackOverflow NWP:
$$\eta_l \in \{10^{-3}, 10^{-2.5}, 10^{-2}, \ldots, 10^{0.5}\}$$
$$\eta \in \{10^{-1.5}, 10^{-1}, 10^{-0.5}, \ldots, 10^1\}$$

D.3 Best performing hyperparameters

In this section, we present, for each optimizer, the best client and server learning rates and values of τ found for the tasks discussed in Section 5. Specifically, these are the hyperparameters used in Figure Figure 1 and table Table 3. The accuracies in Table 3 are obtained using the learning rates in 10 and 11, and the values of τ in Table 12.

Table 10: The base-10 logarithm of the client (η_l) and server (η) learning rate combinations that achieve the accuracies from Table 3. See Appendix D.2 for a full description of the grids.

	FEDADAGRAD		FEDADAM		FEDYOGI		FEDAVGM		FEDAVG	
	η_l	η	η_l	η	η_l	η	η_l	η	η_l	η
CIFAR-100	-½	-½	-1	-³⁄₂	-³⁄₂	-³⁄₂	-1	0	-½	0
EMNIST CR	-1	-1	-⁵⁄₂	-1	-⁵⁄₂	-1	-⁵⁄₂	½	-1	0
SHAKESPEARE	½	-1	½	-1	½	-1	½	-³⁄₂	0	0
STACKOVERFLOW LR	½	1	³⁄₂	½	2	½	2	0	2	0
STACKOVERFLOW NWP	-½	-1	-½	-1	-½	-1	-½	0	-½	½

Table 11: The client learning rate (η_l) and server learning rate (η) that achieve the EMNIST AE accuracies from Table 3. See Appendix D.2 for a full description of the search grid.

	FEDADAGRAD		FEDADAM		FEDYOGI		FEDAVGM		FEDAVG	
	η_l	η	η_l	η	η_l	η	η_l	η	η_l	η
EMNIST AE	10	0.1	5	0.1	5	0.1	1	1	5	1

Table 12: The base-10 logarithm of the parameter τ (as defined in Algorithm 2) that achieve the accuracies from Table 3.

	FEDADAGRAD	FEDADAM	FEDYOGI
CIFAR-100	-1	-3	-3
EMNIST AE	-1	-1	-1
EMNIST CR	-2	-3	-3
SHAKESPEARE	-1	-1	-1
STACKOVERFLOW LR	-5	-5	-5
STACKOVERFLOW NWP	-1	-3	-3

E Comparing client learning rate schedules on EMNIST CR

In Figure 4, we compare the performance of adaptive optimizers on the EMNIST character recognition task using two different types of client learning rate decay schedules: an inverse square root decay, and an exponential decay where the client learning rate decays by a factor of 0.1 every 500 rounds. We also compare to a constant learning rate. Our results show that while both learning rate schedules can offer improvement over constant learning rates, exponential decay tends to better across all optimizers.
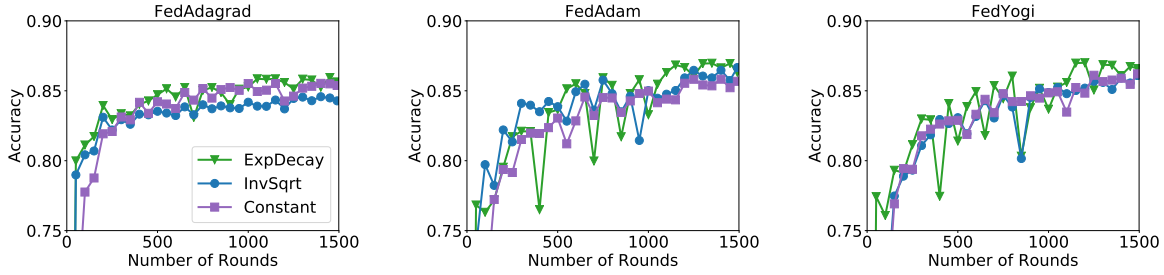
Figure 4: Comparing exponential and inverse square root decay client learning rate schedules to constant client learning rates. We plot the accuracy of adaptive server optimizers with the aforementioned client learning rate scheduless on the EMNIST character recognition task. In all settings, we select 10 clients per round and perform 10 local client epochs.
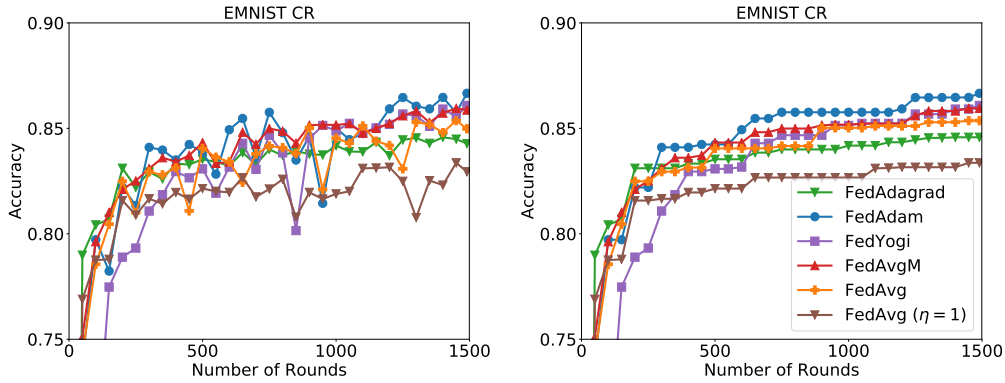

Figure 5: Accuracy of different optimizers on the EMNIST CR task using INVSQRT schedule for the client learning rates. On the left we plot accuracy at a given round, while on the right we plot the maximum accuracy up to a given round. We use 10 local client epochs and 10 clients per round.
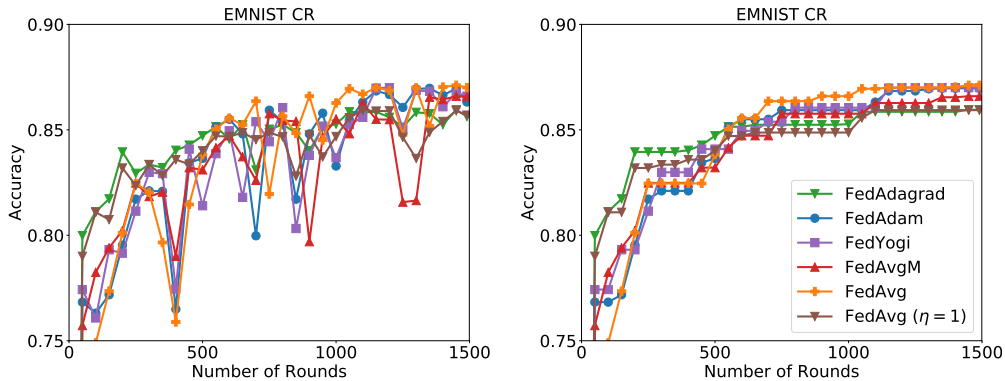

Figure 6: Accuracy of different optimizers on the EMNIST CR task using the EXPDECAY schedule for the client learning rates. On the left we plot accuracy at a given round, while on the right we plot the maximum accuracy up to a given round. We use 10 local client epochs and 10 clients per round.

In Figures 5 and 6, we compare the accuracy of different federated optimizers using the INVSQRT and EXPDECAY learning rate schedules. We also plot the maximum accuracy up to a given round for presentation purposes. We plot the results for two different versions of FEDAVG, one where the learning rate is tuned (FEDAVG) and one where the learning rate is fixed at $\eta = 1$ (corresponding to the description of FEDAVG in (McMahan et al., 2017)). We find that all optimizers benefit from the EXPDECAY schedule when we tune the learning rate.

Our results show that if we were to simply adapt FEDAVG with a client learning rate schedule (fixing a server learning rate of $\eta = 1$), the resulting algorithm does significantly worse than the adaptive optimizers, as well as FEDAVG with a constant but tuned server learning rate. In particular, while FEDAVG with a constant server learning rate of $\eta = 1$ may be sufficient for some tasks, client learning rate schedules potentially increase the need for server learning rate tuning.

F   Creating a Federated CIFAR-100

Overview   We use the Pachinko Allocation Method (PAM) (Li and McCallum, 2006) to create a federated version of the CIFAR-100 dataset. PAM is a topic modeling method in which correlations between words in a vocabulary are represented by a rooted directed acyclic graph (DAG) whose leaves are the vocabulary words. The interior nodes are topics with corresponding Dirichlet distributions over their child nodes. To generate a document, we first sample a multinomial distribution from each interior node's Dirichlet. To sample a word, we begin at the root, and draw a sample over its children from its multinomial distribution. We continue sampling in this way until we reach a leaf node.

To partition CIFAR-100 across clients, we use its coarse-fine label structure. Each image has a fine label (often referred to as just its label) which is a member of a coarse label set. For example, the fine label "seal" is a member of the coarse label set "aquatic mammals". There are 20 coarse labels in CIFAR-100, each with 5 fine labels. We represent this structure as a DAG G, with a single root whose children are the coarse labels. Each coarse label is an interior node whose child nodes are its fine labels. The root node has an associated symmetric Dirichlet distribution with parameter $\alpha = 0.1$ over the coarse labels, and each coarse label has a symmetric Dirichlet distribution with parameter $\beta = 10.0$.

We associate each client to a document. That is, we draw a multinomial distribution from the Dirichlet prior at the root $(\text{Dir}(\alpha))$ and a multinomial distribution from the Dirichlet prior at each coarse label $(\text{Dir}(\beta))$. To create the client dataset, we draw samples from this DAG using PAM. This gives us some fine label leaf node. We draw a random sample with the given fine label, and assign it to the client's dataset. We do this 100 times for 500 distinct training clients.

While more complicated than standard LDA, this approach creates more realistic heterogeneity, as there are correlations between label frequencies for fine labels within the same coarse label set. Intuitively, if a client's dataset has many images of dolphins, it is more likely to also have pictures of whales. We set our Dirichlet parameters α and β to achieve this effect. We use a small α to ensure that clients are likely to focus on a few coarse labels, and we use a large β to increase the likelihood that the clients have multiple fine labels from the same coarse label.

Note that once we sample a fine label, we select an element with that label *without replacement*. This ensures that clients have non-overlapping examples. Suppose we sample a fine label y with coarse label c for client m, and there is only one remaining example (x, c, y) with these labels. We assign (x, c, y) to client m's dataset and remove the y from the DAG G so that future clients cannot sample y. We also remove y from the multinomial distribution θ_c that client m has associated to coarse label c, which we refer to as *renormalization* with respect to y (Algorithm 7). If c has no remaining children after removing y, we remove c from the graph and re-normalize the root multinomial θ_r with respect to c. In future sampling, we perform PAM on this pruned DAG.

Notation and method   Let $\mathcal{C}$ denote the set of fine labels and $\mathcal{Y}$ the set of fine labels, and let $\mathcal{S}$ denote the CIFAR-100 dataset. This consists of examples (x, c, y) where x is an image vector, $c \in \mathcal{C}$ is a coarse label set, and $y \in \mathcal{Y}$ is a fine label with $y \in c$. Given $c \in \mathcal{C}, y \in \mathcal{Y}$, we let $\mathcal{S}_c$ and $\mathcal{S}_y$ denote the set of examples in $\mathcal{S}$ with coarse label c and fine label y. Given a node $v \in G$ (which can either be the root r, a coarse label, or a fine label), we let $|G[v]|$ denote the set of children of v in G. For $\gamma \in \mathbb{R}$, let $\text{Dir}(\gamma, k)$ denote the symmetric Dirichlet distribution with k categories. Let M denote the desired number of clients, N denote the desired number of examples per client, and D_m denote the dataset for client $m \in \{1, \cdots, M\}$. A full description of our method for creating a federated CIFAR-100 is given in Algorithm 6. For our experiments, we use $N = 100, M = 500, \alpha = 0.1, \beta = 10$.

Algorithm 6 Creating a federated CIFAR-100

> Input: $N, M \in \mathbb{Z}_{>0}, \alpha, \beta \in \mathbb{R}_{\geq 0}$
> **for** $m = 1, \cdots, M$ **do**
>   Sample $\theta_r \sim \text{Dir}(\alpha, |G[r]|)$
>   **for** $c \in \mathcal{C} \cap G[r]$ **do**
>   Sample $\theta_c \sim \text{Dir}(\beta, |G[c]|)$
> $D_m = \emptyset$
>   **for** $n = 1, \cdots N$ **do**
>   Sample $c \sim \text{Multinomial}(\theta_r), y \sim \text{Multinomial}(\theta_c)$
>   Select $(x, c, y) \in \mathcal{S}$ uniformly at random
> $D_m = D_m \cup \{(x, c, y)\}, \mathcal{S} = \mathcal{S} \backslash \{(x, c, y)\}$
>   **if** $\mathcal{S}_y = \emptyset$ **then**
> $G = G \backslash \{y\}, \theta_c = \text{RENORMALIZE}(\theta_c, y)$
>   **if** $\mathcal{S}_c = \emptyset$ **then**
> $G = G \backslash \{c\}, \theta_r = \text{RENORMALIZE}(\theta_r, c)$

Algorithm 7 RENORMALIZE

> Initialization: $\theta = (p_1, \ldots, p_K), i \in [K]$
> $a = \sum_{k \neq i} p_k$
> **for** $k \in [K], k \neq i$ **do**
> $p'_k = p_k / a$
> Return $\theta' = (p'_1, \cdots p'_{i-1}, p'_{i+1}, \cdots, p'_K)$

In Figure 7, we plot the distribution of unique labels among the 500 training clients. Each client has only a fraction of the overall labels. Moreover, there is some variance to the number of unique clients, with most having between 20 and 30, and some having over 40. Other client datasets have very small numbers of unique labels. While this is primarily an artifact of performing without replacement sampling, this helps increase the heterogeneity of the dataset in a way that reflects practical concerns. In many settings, clients may only have a few types of labels in their dataset.
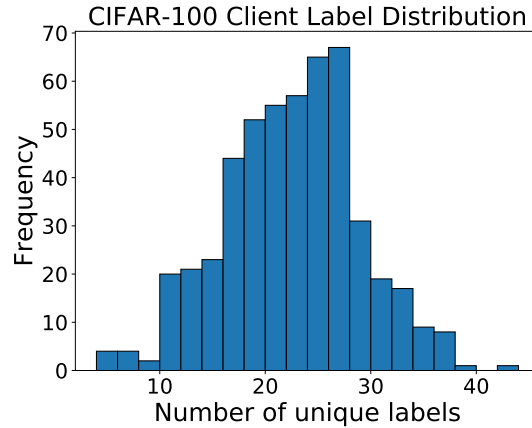

Figure 7: The distribution of the number of unique labels among training clients in our federated CIFAR-100 dataset.